Computational Journal of Mathematical and Statistical Sciences
4(1), 348–378
DOI:10.21608/cjmss.2025.353923.1107
https://cjmss.journals.ekb.eg/

Bayesian and E-Bayesian Estimation of Gompertz Distribution in Stress-Strength Reliability Model under Partially Accelerated Life Testing

Amal S. Hassan[1] **and Ahmed M. Abd Elghaffar**[2,3*]

[1] Department of Mathematical Statistics, Faculty of Graduate Studies for Statistical Research, Cairo University, 12613 Giza, Egypt; amal52_soliman@cu.edu.eg.

[2] Department of Mathematical Statistics, Faculty of Graduate Studies for Statistical Research, Cairo University, 12613 Giza, Egypt; 12422018457111@pg.cu.edu.eg.

[3] Offsite Sector, Central Bank of Egypt, 11511 Cairo, Egypt; ahmed.abdelghaffar@cbe.org.eg

* **Correspondence:** 12422018457111@pg.cu.edu.eg

Abstract: A reliability experiment is a crucial determinant of a component's success, as it simulates the effects of aging and usage by exposing the component in a system to higher levels of stress or wear. Consequently, assessments of the component's performance and its capacity to satisfy consumers are conducted. This study aims to estimate the stress-strength inequality function $R = P(Y < X)$ after subjecting it to a step-stress partially accelerated life test, which acts as a secondary test by exposing the component to more extreme conditions than usual. The strength variable (X) and stress variable (Y) are assumed to be independent random variables following the Gompertz distribution. The maximum likelihood method was used to estimate the model parameters and the stress-strength parameter R. Two alternative estimation techniques were utilized, specifically the Bayesian method proposing gamma priors for the model's parameters and E-Bayesian estimation suggesting beta priors for the hyperparameters. Furthermore, Lindley's approximation method and Markov Chain Monte Carlo simulation were utilized with both the squared error and the precautionary loss functions to derive Bayesian and E-Bayesian estimators. Interval estimation methods such as asymptotic confidence intervals, Bayes, and expected Bayes credible intervals were discussed. A simulation study and real-data application were employed to evaluate the proposed estimating methods that have been developed in addition to verifying the accuracy of the results.

Keywords: Stress-strength reliability, Step-stress partially accelerated life test, Gompertz distribution, E-Bayesian estimation, Asymptotic confidence intervals.
Mathematics Subject Classification: 60E05, 62E10, 62F10.
Received: 18 January 2025; Revised: 29 March 2025; Accepted: 30 March 2025; Online: 2 April 2025.

1. Introduction

1.1. Background

The stress-strength reliability model (SSRM) has been widely used in various fields such as engineering, economics, risk assessment, quality control, health, and technology. For highly reliable components where failures are rare occurrences, it is exceedingly difficult to obtain a failure sample. Thus, to gather data, it is essential to execute an accelerated life test (ALT) or partially ALT (PALT) throughout the phases of development and production. The fundamental concept underlying ALT or PALT involves subjecting the components to severe degrees of operational and environmental conditions that are beyond their average exposure, with the intent of estimating the behavioral attributes of the components. Progressive stress, step stress, and constant stress can be utilized in the evaluation. The ALT assumes a knowledge relationship between component lifetimes and stress. When such a relation is absent, PALT is the best for representing the model's parameters. Currently, a combination of the SSRM and the PALT was developed to examine components' strength through stress, ensuring that the experiment would be accomplished in a shorter time. Four basic models were used mainly to illustrate the impact of stress level variations on components' residual lifetime during accelerated testing: the tampered random variable model, the tampered failure rate (TFR) model, the linear cumulative exposure model and the cumulative exposure model.

Several PALT models have been thoroughly studied. For example, Srivastava and Mittal [47] considered the optimal design of the SSPALT, assuming that the life of the items follows a truncated logistic distribution truncated at point zero. Inferential procedures involving the model parameters and the acceleration factor were studied. Abushal and Soliman [1] assumed that the lifetime of the items follows the two-parameter Pareto distribution of the second kind. PALT based on progressively Type II censoring scheme (CS) was considered, as well as maximum likelihood estimators, asymptotic confidence intervals (ACIs), two bootstrap confidence intervals (CIs), and Bayes estimators for the parameters were derived. Kamal et al. [34] considered the Nadarajah-Haghighi distribution when the SSPALT model was under adaptive Type II progressively hybrid CS. The maximum likelihood estimators of the model parameters and the acceleration factor were derived, and the Fisher information matrix (FIM) was constructed to produce the ACIs. The estimation of constant PALT for the Weibull distribution of the competing risks model was provided by Hassan et al. [31]. For recent studies, the reader can refer to [3, 5, 6, 7, 22, 32].

The SSRM was initially proposed by Birnbaum [14], which was further developed by Birnbaum and McCarty [15]. SSRM can be described as a technique for assessing the reliability of a component by comparing two sets of random variables, X and Y. In this simplified situation, the component would fail if the applied stress exceeded its strength ($Y > X$), and vice versa. The SSRM is defined as the probability of avoiding failure $P(Y < X)$ expressed as follows:

$$R = \int_0^\infty f(x) G_Y(x) dx.$$

Considering SSRM, Mokhlis [41] discussed the reliability of a system when both strength and stress are independent and non-identical Burr Type III distributions of random variables. Asgharzadeh et al. [10] obtained maximum likelihood estimators and Bayesian estimators (BEs) of the stress–strength parameter (SSP) R when X and Y are independent random variables from two generalized logistic distributions. For more recent studies, see [4, 8, 25, 29, 30, 38, 40].

Recently, Çetinkaya [18] introduced SSRM in the presence of PALT. This test design combines two distinct forms of tests that were hierarchically imposed on the components of a system. The developed model includes two stresses: the main stress, denoted by SSRM, and the PALT, respectively. In addition, maximum likelihood estimators with their ACIs and BEs with their highest posterior density credible intervals were provided. The model was formulated according to the following equation:

$$R = \int_0^\tau \int_0^x f_1(x)dG(y)dx + \int_\tau^\infty \int_0^x f_2(x)dG(y)dx, \tag{1.1}$$

where,

$f_1(x)$ and $f_2(x)$ are the probability density functions (PDFs) of the strength variable X at normal use conditions and higher stress levels when implementing PALT, respectively.

$G(y)$ is the cumulative distribution function (CDF) of the strength variable Y, under normal use conditions, and τ is a pre-fixed assigned transition time, at which stress shifts to a higher level.

The TFR model was first proposed by Bhattacharrya and Soejoeti [13], and then generalized by Madi [37]. Acceleration of failure demonstrates the changes that take place in the hazard rate function when the stress level changs from a lower to a higher level as the load is subjected to a predetermined sequence of loads denoted by $\mathcal{L}_i(i = 0, 1, ..., q-g)$. Thus, the hazard rate function $H(t)$ of the component at time t can be represented as follows:

$$H(t) = H_i(t) = \lambda_i(\mathcal{L}_i)H_\circ(t), \qquad \tau_{i-1} \le t < \tau_i,$$

where,

q: the total number of components in the system,

g: the minimum number of components required for successful operation,

$\mathcal{L}_i$ is the number of loads with sequence $(i = 0, 1, ..., q - g)$ occurring at time $\tau_1, \tau_2, ..., \tau_{q-g}$, at $\tau_0 = 0$,

$H_0(t)$: the hazard rate at the lower load $\mathcal{L}_0$,

λ_i is the acceleration factor, which is considered to be a function of the loads $\mathcal{L}_i$ at time t.

According to this model, the mathematical expression of the TFR model is shown below:

$$H(t) = \begin{cases} H_{TFR}(t), & t \le \tau. \\ \lambda H_{TFR}(t), & \tau < t. \end{cases}$$

Applying TFR model, the CDF of the samples can be expressed as follows:

$$F(x) = \begin{cases} F_1(x), & x \le \tau, \\ F_2(x) = 1 - (1 - F_1(\tau))^{1-\lambda}(1 - F_1(x))^\lambda, & \tau < x, \end{cases} \tag{1.2}$$

where $F_1(x) = 1 - e^{-\int_0^x H_{TFR}(x)d(x)}$ and the acceleration factor $\lambda > 1$.

1.2. Related Works

The combination of SSRM and PALT improves the reliability evaluation of the product under both severe and normal conditions, while enabling accelerated data collection using higher levels of stress for a limited period of time. Thus, it works to reduce testing, duration, and costs while preserving the integrity of the result. In addition to what has been discussed by Çetinkaya [18] which has been recognized as the pioneer study in the introduction of SSRM in the presence of PALT. Quite a few studies addressed this notion; for example, El-Sagheer et al. [24] estimated the SSRM when the strength variable is used along with the SSPALT under the assumption that the stress and strength random variables have a common shape parameter and follow the Weibull distribution. Sarhan and Tolba [46] provided maximum likelihood estimators and BEs of $R = P(Y < X)$ in the context of the SSPALT when both variables X and Y follow an exponential distribution. Yousef et al. [51] derived maximum likelihood estimators and BEs of $R = P(Y < X)$ considering the progressive type II CS while applying SSRM based on the SSPALT. Temraz [48] used the maximum likelihood estimators and ACIs methods to estimate the fuzzy multicomponent SSP in the presence of the PALT, assuming that the data follow the inverse Weibull distribution.

1.3. Motivation of the Study

The efficacy of the SSRM in the presence of PALT can be explained as the development of a more conservative framework that incorporates two distinct types of tests that occur hierarchically throughout a lifetime test. This approach for evaluating a component's lifetime is used not only to demonstrate reliability and lifetime but also to speed up the production process, thereby reducing the time required to bring the component to market. Furthermore, enhancing product reliability through such testing significantly increases customer loyalty and increases corporate revenue. The rationale for our choice to implement the SSRM under PALT in our study is rooted in its extensive use in several fields and the previously recognized advantageous characteristics it possesses. The Gompertz distribution (GD) can show positive or negative skewness. It is a generalized form of exponential distribution and was historically introduced by Gompertz [27]. GD is widely documented in the literature for its practical uses in several domains, primarily in the area of analyzing data related to the duration of events or lifetimes; see [33]. Survival studies have been conducted in some sciences, such as gerontology [16], computer science [44], biology [50], sociology [20], marketing science [11], and biotechnology [49]. Multiple studies have used GD in modeling reliability. Saraçoğlu and Kaya [45] obtained the maximum likelihood estimators and CIs of the SSRM while considering the probability estimation problem $R = P(Y < X)$, assuming that the stress variable Y and the strength variable X follow the GD. Kumar and Vaish [35] studied the problem of SSRM, assuming that stress follows the GD and strength follows a power function distribution. Asadi et al. [9] discussed the GD under the constant-stress PALT model based on adaptive Type II progressive hybrid CS.

The present study discusses the parameter point estimators and the accelerated factor using maximum likelihood estimation (MLE) and Bayesian estimation methods. Furthermore, interval estimators were created, including ACIs, Bayesian credible intervals (BCIs), and bootstrap CIs. Two distinct estimation techniques, referred to as E-Bayesian estimation and E-Bayesian credible intervals (E-BCIs) have been adopted, which have never been utilized before in similar studies. Our efforts will be summarized as follows:

1. Offer an in-depth description of the stress-strength model $P(Y < X)$. This system commences under normal conditions for both variables X and Y, whereby the strength component X is exposed to the stress component Y. If the system does not fail before the predetermined time τ, the strength variable X is running at an acceleration factor λ. Assuming both stress and strength variables follow GD, where $Y \sim$ GD (α), $X \sim$ GD, (θ) and when a higher stress level is experienced using PALT, $X \sim$ GD (θ, λ).

2. Given the complete sample size, MLE, BEs, E-Bayesian estimators (E-BEs), ACIs, in addition to BCIs and E-BCIs are obtained for the SSP R.

3. Obtain the BEs and E-BEs of the SSP R with informative (INF) and non-informative (NINF) priors using the Lindley approximation method and Markov chain Monte Carlo (MCMC) simulation, which is represented by the Gibbs sampling algorithm, considers two separate loss functions (LFs), represented by the squared error loss function (SELF) and the precautionary loss function (PLF).

4. Evaluate and compare the efficacy of various estimation methods by conducting simulation studies with different sample sizes to determine how several estimates perform in terms of accuracy, reliability, and unbiasedness. Finally, a real-world dataset is provided to support the theoretical conclusions.

The structure of the paper is as follows. Section 2 provides an extensive description of the SSRM under SSPALT. The development of maximum likelihood estimators for the SSP is presented in Section 3. In Section 4, the BEs of the model's parameters are computed under SELF and PLF using the Lindley approximation and the Gibbs sampling algorithm. The E-BE of the SSP has been computed using the SELF and PLF approaches, utilizing the Lindley technique and the Gibbs sampling algorithm in Section 5. In Section 6, interval estimation, including ACIs, BCIs, and E-BCIs, is considered. In Section 7, simulation methodology has been implemented to assess and compare the effectiveness of various estimation methodologies. In Section 8, the proposed estimation methodologies have been used to examine real data. The outcomes of this study are presented in Section 9.

2. Model Description

According to El-Gohary et al. [23], the distribution of our interest in this study is mathematically considered a special case of generalized GD, where $X \sim \mathrm{GD}(\theta)$ with parameter θ. Subsequently, the CDF and the PDF of the GD are ascertained by the following formula:

$$F(x;\theta) = 1 - e^{-\theta(e^{x}-1)}; \qquad \theta, x > 0, \tag{2.1}$$

and

$$f(x;\theta) = \theta e^{x-\theta(e^{x}-1)}; \qquad \theta, x > 0.$$

This study's main contribution is to look at how reliable a system is when the SSRM and SSPALT were presented. The model assumes that the two underlying variables follow an GD in the context of complete data.

Consider X and Y be two independent random variables that follow the GD with parameters θ and α, respectively. The CDF of the strength variable under SSPALT is obtained by inserting Equation (2.1) in Equation (1.2) as follows:

$$F(x) = \begin{cases} F_1(x;\theta) = 1 - e^{-\theta(e^x-1)}\ ; & x \leq \tau, \\ F_2(x;\theta,\lambda) = 1 - e^{-\theta[\lambda(e^x-1)+(1-\lambda)(e^\tau-1)]}\ ; & \tau < x. \end{cases} \tag{2.2}$$

The corresponding PDF is defined as follows:

$$f(x) = \begin{cases} f_1(x;\theta) = \theta e^{x-\theta(e^x-1)}\ ; & x \leq \tau. \\ f_2(x;\theta,\lambda) = \theta\lambda e^{x-\theta[\lambda(e^x-1)+(1-\lambda)(e^\tau-1)]}\ ; & \tau < x. \end{cases} \tag{2.3}$$

The PDF and CDF of the primary stress Y are provided by

$$\begin{array}{ll} g(y;\alpha) = \alpha e^{y-\alpha(e^y-1)}; & y > 0 \\ G(y;\alpha) = 1 - e^{-\alpha(e^y-1)}; & y > 0 \end{array}. \tag{2.4}$$

The hazard function $H_1(x;\theta)$ and the survival function $\bar{F}_1(x;\theta)$, which incorporate the strength variable X under the normal used condition, are defined as follows:

$$\begin{array}{ll} H_1(x;\theta) = \theta e^x; & x \leq \tau \\ \bar{F}_1(x;\theta) = e^{-\theta(e^x-1)}; & x \leq \tau \end{array}. \tag{2.5}$$

SSPALT's hazard function $H_2(x;\theta)$ is derived by multiplying $H_1(x;\theta)$ by an acceleration factor λ, where $\lambda > 1$, when stress is raised to a specific time τ. This leads to the following formula:

$$H_2(x;\theta,\lambda) = \theta\lambda e^x; \qquad \tau < x. \tag{2.6}$$

Considering the formula $\bar{F}_2(x;\theta) = \int_0^x H_2(x;\theta,\lambda)dx$, the survival function can be obtained as given below:

$$\bar{F}_2(x;\theta,\lambda) = e^{-\theta[\lambda(e^x-1)+(1-\lambda)(e^\tau-1)]}; \qquad \tau < x. \tag{2.7}$$

Within the framework of the SSRM involving the application of the SSPALT, the strength of the variable X represented by its PDF $f(x)$ and CDF $F(x)$ has been investigated, considering the impacts of the primary stress variable Y characterized by its PDF $g(y)$ and CDF $G(y)$. Thus, the SSP R of the above system is calculated by plugging Equation (2.3) and the PDF of the stress variable Y mentioned in Equation (2.4) into Equation (1.1) as shown below:

$$R = \alpha\theta \int_0^\tau \int_0^x e^{x-\theta(e^x-1)} e^{y-\alpha(e^y-1)} dydx + \alpha\theta\lambda \int_\tau^\infty \int_0^x e^{x-\theta[\lambda(e^x-1)+(1-\lambda)(e^\tau-1)]} e^{y-\alpha(e^y-1)} dydx.$$

After simplification, the SSP R is given by:

$$R = \frac{\alpha}{\theta+\alpha} + \frac{\theta\alpha(1-\lambda)}{(\theta+\alpha)(\theta\lambda+\alpha)} e^{-(\theta+\alpha)(e^\tau-1)}. \tag{2.8}$$

In cases where acceleration is not taken into concern and just GD under SSRM is considered, it is evident that the reliability of a simple stress-strength system may be expressed in the formula (2.8) when λ= 1.

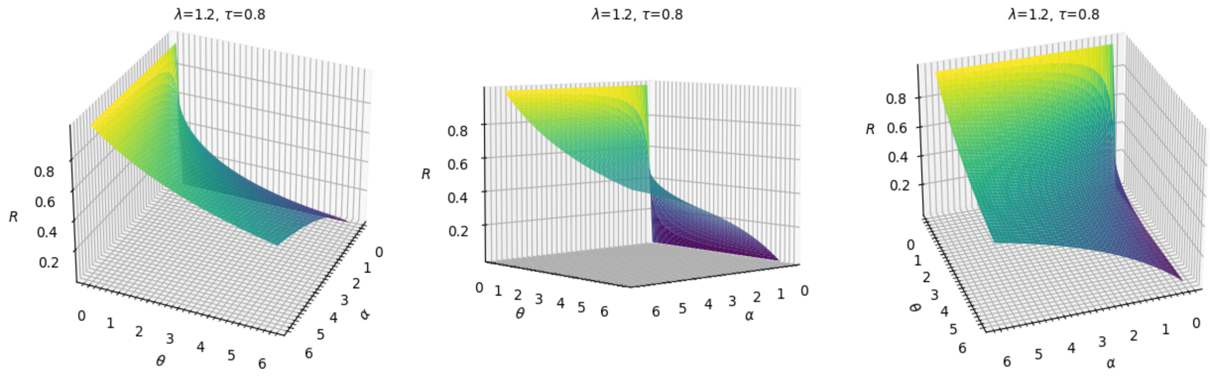

Figure 1. The stress–strength parameter R under SSPALT

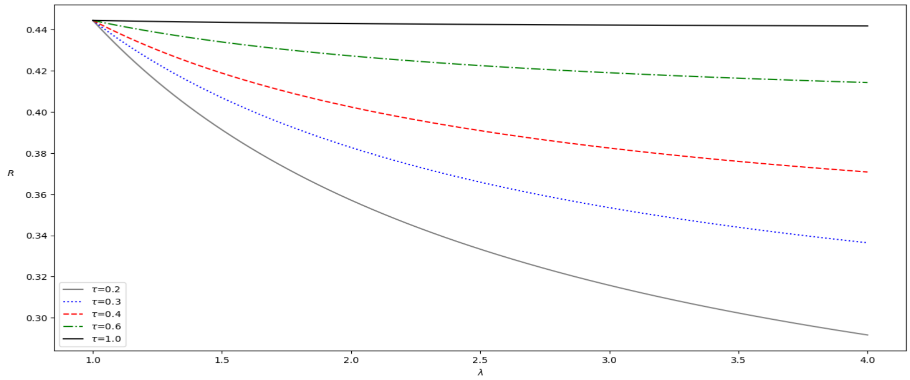

Figure 2. Actual R values with increasing τ points for various λ values in the case of $\alpha = 1.2$ and $\theta = 1.5$

The diagram illustrated above, referred to as Figure 1, presents a three-dimensional graphical depiction of the SSP R. The model highlighted the effect of different values of α and θ while keeping both λ and τ constant, where ($\lambda = 1.2$ and $\tau = 0.8$). (i) As the value of θ increases, there is a corresponding decrease in the SSP. (ii) As the value of α grows, the system becomes more reliable.

The graphical representation in Figure 2 shows a direct relationship between R and stress change time τ, while keeping the acceleration factor λ constant. The SSP decreases noticeably as the acceleration factor λ rises, as seen in Figure 3. As illustrated, when λ=1, the SSPALT exerts minimal influence on the SSP R.

3. MLE of R's Parameters

Suppose that $(x_1, x_2, ..., x_n)$ represent the observed values of the strength X, and $(y_1, y_2, ..., y_m)$ denote the observed values of the stress Y. Both the stress and strength random samples are independent and selected from the Gompertz population. The MLE is used to get point estimates of the unknown parameters θ, α, and λ using Equation (2.3) and the PDF included in Equation (2.4) as follows:

$$L(\Theta|\underline{x}, \underline{y}) = \prod_{i=1}^{r} f_1(x_i|\theta) \prod_{i=r+1}^{n} f_2(x_i|\theta, \lambda) \prod_{j=1}^{m} g(y_j|\alpha), \tag{3.1}$$

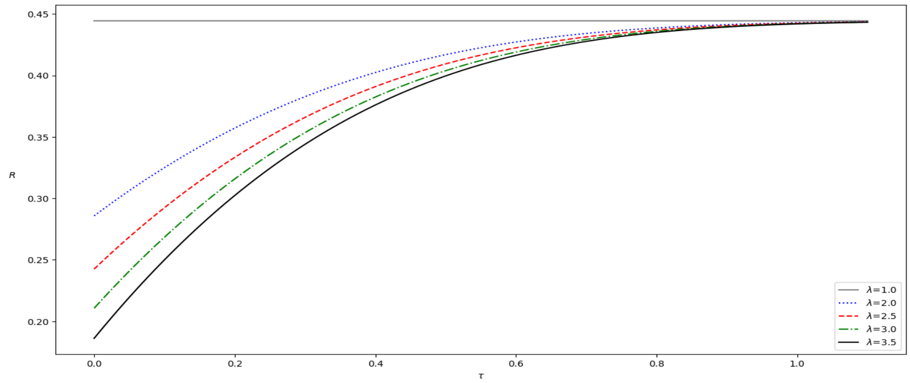

Figure 3. Actual R values with increasing λ points for various τ values in the case of $\alpha = 1.2$ and $\theta = 1.5$

where $\Theta \equiv (\theta, \alpha, \lambda)$, $x_r \le \tau < x_{r+1}$, and R is the total number of items that failed before the occurrence of the predetermined time τ.

Using Equation (3.1), the likelihood function is given as follows:

$$L(\Theta|\underline{x}, \underline{y}) = \theta^n \alpha^m \lambda^{n-r} \prod_{i=1}^{r} e^{x_i - \theta(e^{x_i}-1)} \prod_{i=r+1}^{n} e^{x_i - \theta[\lambda(e^{x_i}-1)+(1-\lambda)(e^{\tau}-1)]} \prod_{j=1}^{m} e^{y_j - \alpha(e^{y_j}-1)}. \tag{3.2}$$

Thus, the corresponding log-likelihood function is given by:

$$\begin{aligned} \ell(\Theta|\underline{x}, \underline{y}) \propto\ & n\log(\theta) + m\log(\alpha) + (n-r)\log(\lambda) - \theta \sum_{i=1}^{r}(e^{x_i} - 1) - \theta\lambda \sum_{i=r+1}^{n}(e^{x_i} - 1) - (n-r)\theta \\ & \times (1-\lambda)(e^{\tau} - 1) - \alpha \sum_{j=1}^{m}(e^{y_j} - 1). \end{aligned} \tag{3.3}$$

To obtain maximum likelihood estimators of the vector parameter Θ, the log-likelihood function needs to be maximized separately for each parameter. From Equation (3.3), it is clear that the MLE of θ, α, and λ can be obtained by solving the following three equations.

$$\frac{\ell(\Theta|\underline{x}, \underline{y})}{\partial\theta} = \frac{n}{\theta} - \sum_{i=1}^{r}(e^{x_i} - 1) - \lambda \sum_{i=r+1}^{n}(e^{x_i} - e^{\tau}) - (n-r)(e^{\tau} - 1) = 0, \tag{3.4}$$

$$\frac{\ell(\Theta|\underline{x}, \underline{y})}{\partial\alpha} = \frac{m}{\alpha} - \sum_{j=1}^{m}(e^{y_j} - 1) = 0, \tag{3.5}$$

$$\frac{\ell(\Theta|\underline{x}, \underline{y})}{\partial\lambda} = \frac{n-r}{\lambda} - \theta \sum_{i=r+1}^{n}(e^{x_i} - e^{\tau}) = 0. \tag{3.6}$$

From Equation (3.5), the MLE of α can be determined by solving the following equation.

$$\hat{\alpha} = \frac{m}{\sum_{j=1}^{m}(e^{y_j} - 1)}. \tag{3.7}$$

Given Equation (3.4), the MLE of θ, say $\hat{\theta}(\lambda)$, can be solved numerically using a numerical iterative technique as follows.

$$\hat{\theta}(\lambda) = \frac{n}{\sum_{i=1}^{r}(e^{x_i} - 1) + \lambda \sum_{i=r+1}^{n}(e^{x_i} - e^{\tau}) + (n-r)(e^{\tau} - 1)}. \tag{3.8}$$

Therefore, the MLE of λ can be obtained by inserting outcomes from $\hat{\theta}(\lambda)$ in the non-linear Equation (3.6) as follows.

$$\frac{n-r}{\lambda} - \frac{n\sum_{i=r+1}^{n}(e^{x_i} - e^{\tau})}{\sum_{i=1}^{r}(e^{x_i} - 1) + \lambda \sum_{i=r+1}^{n}(e^{x_i} - e^{\tau}) + (n-r)(e^{\tau} - 1)} = 0. \tag{3.9}$$

Using the iteration technique, the MLE of λ is obtained by solving numerically the non-linear Equation (3.9), then substituting the value of $\hat{\lambda}$ in Equation (3.8) to obtain $\hat{\theta}$. Finally, by using the invariance property, the maximum likelihood estimation of R, represented by $\hat{R}_{ML}$, is as follows after substituting $\hat{\theta}(\lambda)$, $\hat{\alpha}$, and $\hat{\lambda}$ in Equation (2.8).

$$\hat{R}_{ML} = \frac{\hat{\alpha}}{\hat{\theta}(\lambda) + \hat{\alpha}} + \frac{\hat{\theta}(\lambda)\hat{\alpha}(1-\hat{\lambda})}{(\hat{\theta}(\lambda) + \hat{\alpha})(\hat{\theta}(\lambda)\hat{\lambda} + \hat{\alpha})} e^{-(\hat{\theta}(\lambda)+\hat{\alpha})(e^{\tau}-1)}. \tag{3.10}$$

4. Bayesian Estimation of *R*

In this section, the SSP R using the Lindley approximation method will be considered. Globally, when analyzing an estimate from a Bayesian perspective, the key factor is to define prior distributions for the unknown parameters. When there is a lack of relevant background data, it is customary to utilize NINF priors; refer to Carlin and Louis [17] for more details. In order to derive BEs for the unknown parameters, it is assumed that both parameters θ and α have independent gamma priors, while the parameter λ has an NINF prior. The joint prior of the unknown parameters θ, α, and λ is:

$$S(\Theta) \propto \frac{\theta^{a_1-1}\alpha^{a_2-1}}{\lambda} e^{-\left(\theta b_1 + \alpha b_2\right)} \qquad , a_1, b_1, a_2, b_2 > 0; \quad \lambda > 1. \tag{4.1}$$

The joint posterior density functions of θ, α, and λ are obtained using the following mathematical equation:

$$\pi(\Theta|\underline{x}, \underline{y}) = \frac{L(\Theta|\underline{x}, \underline{y})S(\Theta)}{\int_{\Theta} L(\Theta|\underline{x}, \underline{y})S(\Theta)d\Theta}, \tag{4.2}$$

where $d\Theta = d\theta d\alpha d\lambda$. By substituting $L(\Theta|\underline{x}, \underline{y})$ and $S(\Theta)$ in Equation (4.2), the following joint posterior $\pi(\Theta|\underline{x}, \underline{y})$ has been obtained:

$$\begin{aligned}\pi(\Theta|\underline{x}, \underline{y}) = {} & K\theta^{n+a_1-1}\alpha^{m+a_2-1}\lambda^{n-r-1}e^{-\left(\theta b_1 + \alpha b_2\right)} e^{-\theta\sum_{i=1}^{r}(e^{x_i}-1)} e^{-\theta[\lambda\sum_{i=r+1}^{n}(e^{x_i}-e^{\tau})+(n-r)(e^{\tau}-1)]} \\ & \times e^{-\alpha\sum_{j=1}^{m}(e^{y_j}-1)},\end{aligned} \tag{4.3}$$

where,

$$K^{-1} = \int_1^{\infty}\int_0^{\infty}\int_0^{\infty} \theta^{n+a_1-1}\alpha^{m+a_2-1}\lambda^{n-r-1}e^{-\left(\theta b_1 + \alpha b_2\right)} e^{-\theta\sum_{i=1}^{r}(e^{x_i}-1)} e^{-\theta[\lambda\sum_{i=r+1}^{n}(e^{x_i}-e^{\tau})+(n-r)(e^{\tau}-1)]}$$

$$\times e^{-\alpha \sum_{j=1}^{m}(e^{y_j}-1)} d\theta d\alpha d\lambda.$$

Assigning an appropriate LF is crucial for Bayesian parameter estimation. Consequently, LFs that demonstrate both symmetry and asymmetry have been considered. The SELF is widely considered the most often employed approach for estimating problems since it gives equal weight to losses caused by both overestimation and underestimation. The Bayes estimate of the parametric function of interest, say $R(\Theta)$ under SELF, is obtained by $L(\hat{R}(\Theta), R(\Theta)) = (\hat{R}(\Theta) - R(\Theta))^2$. Although this assumption may not be inappropriate for all estimating issues, thus, Norstrom [42] provided a definition for an alternate asymmetric LF called PLF, denoted as $L(\hat{R}(\Theta), R(\Theta)) = \frac{(\hat{R}(\Theta)-(R(\Theta))^2}{\hat{R}(\Theta)}$. The PLF avoids underestimating problems by approaching infinitely close to the origin.

4.1. Bayesian estimation of R using Lindley approximation method

Due to the complexity of analytically computing the stated equations, the Lindley approximation method, introduced by Lindley [36], which approaches the ratio of the integrals as a whole and produces a single numerical result, was proposed for obtaining the BEs. The ratio of integrals that arises in Bayesian analysis is expressed as

$$\hat{R}_L(\Theta) = \mathbb{E}(R(\Theta)|\underline{x}, \underline{y}) = \frac{\int_\Theta R(\Theta) e^{\ell(\Theta|\underline{x},\underline{y})\rho(\Theta|\underline{x},\underline{y})} d\Theta}{\int_\Theta e^{\ell(\Theta|\underline{x},\underline{y})\rho(\Theta|\underline{x},\underline{y})} d\Theta}, \tag{4.4}$$

where $\hat{R}_L(\Theta)$ represents the Bayes estimate of the parametric function of interest utilizing Lindley's approximation, $\ell(\Theta|\underline{x}, \underline{y})$ is the log-likelihood function, and $\rho(\Theta|\underline{x}, \underline{y})$ is the log of the joint prior of Θ. To approximate Lindley's technique, we employ a Taylor series considering the MLE of $(\theta, \alpha, \lambda)$ to expand the log of the joint prior $\rho(\Theta|\underline{x}, \underline{y})$ and the log-likelihood function $\ell(\Theta|\underline{x}, \underline{y})$ in Equation (4.4).

$$\hat{R}_L(\Theta) = \mathbb{E}(R(\Theta) \mid \underline{x}, \underline{y}) = \hat{R}_{ML} + \frac{1}{2}\sum_{i,j=1}^{q} [R_{ij} + 2R_i\rho_j]\sigma_{ij} + \frac{1}{2}\sum_{i,j,k,l=1}^{q} \ell R_k \sigma_{ij}\sigma_{kl},$$

where q is the total number of parameters; $R_i = \frac{\partial R}{\partial \Theta_i}$; $R_{ij} = \frac{\partial^2 R}{\partial\Theta_i\partial\Theta_j}$; $\ell_{ij} = \frac{\partial^2 \ell}{\partial\Theta_i\partial\Theta_j}$; $\ell_{ijk} = \frac{\partial^3 \ell}{\partial\Theta_i\partial\Theta_j\partial\Theta_k}$; $\rho_j = \frac{\partial \rho}{\partial \Theta_j}$; and σ_{ij} represents the $(i, j) - th$ element of the ℓ_{ij} inverse matrix.

In the case of the three parameters $(\theta, \alpha, \lambda)$, for $i = j = k = (1, 2, 3) \equiv (\theta, \alpha, \lambda)$. Given $(\Theta_1 \equiv \theta, \Theta_2 \equiv \alpha, \Theta_3 \equiv \lambda)$, the approximation of the posterior expectation is expressed as follows:

$$\begin{aligned}
\hat{R}_L(\Theta) = \hat{R}_{ML} + \frac{1}{2}\Big[&(R_{\theta\theta} + 2R_\theta\rho_\theta)\sigma_{\theta\theta} + (R_{\alpha\theta} + 2R_\alpha\rho_\theta)\sigma_{\alpha\theta} + (R_{\lambda\theta} + 2R_\lambda\rho_\theta)\sigma_{\lambda\theta} \\
&+ (R_{\theta\alpha} + 2R_\theta\rho_\alpha)\sigma_{\theta\alpha} + (R_{\lambda\alpha} + 2R_\lambda\rho_\alpha)\sigma_{\lambda\alpha} + (R_{\alpha\alpha} + 2R_\alpha\rho_\alpha)\sigma_{\alpha\alpha} \\
&+ (R_{\theta\lambda} + 2R_\theta\rho_\lambda)\sigma_{\theta\lambda} + (R_{\alpha\lambda} + 2R_\alpha\rho_\lambda)\sigma_{\alpha\lambda} + (R_{\lambda\lambda} + 2R_\lambda\rho_\lambda)\sigma_{\lambda\lambda}\Big] \\
&+ \frac{1}{2}\Big[\Lambda_1(R_\theta\sigma_{\theta\theta} + R_\alpha\sigma_{\theta\alpha} + R_\lambda\sigma_{\theta\lambda}) + \Lambda_2(R_\theta\sigma_{\alpha\theta} + R_\alpha\sigma_{\alpha\alpha} + R_\lambda\sigma_{\alpha\lambda}) \\
&+ \Lambda_3(R_\theta\sigma_{\lambda\theta} + R_\alpha\sigma_{\lambda\alpha} + R_\lambda\sigma_{\lambda\lambda})\Big],
\end{aligned} \tag{4.5}$$

where, $\Lambda_1 = \sigma_{\theta\theta}\ell_{\theta\theta\theta} + 2\sigma_{\theta\alpha}\ell_{\theta\alpha\theta} + 2\sigma_{\theta\lambda}\ell_{\theta\lambda\theta} + 2\sigma_{\alpha\lambda}\ell_{\alpha\lambda\theta} + \sigma_{\alpha\alpha}\ell_{\alpha\alpha\theta} + \sigma_{\lambda\lambda}\ell_{\lambda\lambda\theta}$,

$$\Lambda_2 = \sigma_{\theta\theta}\ell_{\theta\theta\alpha} + 2\sigma_{\theta\alpha}\ell_{\theta\alpha\alpha} + 2\sigma_{\theta\lambda}\ell_{\theta\lambda\alpha} + 2\sigma_{\alpha\lambda}\ell_{\alpha\lambda\alpha} + \sigma_{\alpha\alpha}\ell_{\alpha\alpha\alpha} + \sigma_{\lambda\lambda}\ell_{\lambda\lambda\alpha},$$

$$\Lambda_3 = \sigma_{\theta\theta}\ell_{\theta\theta\lambda} + 2\sigma_{\theta\alpha}\ell_{\theta\alpha\lambda} + 2\sigma_{\theta\lambda}\ell_{\theta\lambda\lambda} + 2\sigma_{\alpha\lambda}\ell_{\alpha\lambda\lambda} + \sigma_{\alpha\alpha}\ell_{\alpha\alpha\lambda} + \sigma_{\lambda\lambda}\ell_{\lambda\lambda\lambda}.$$

The $\hat{R}_{LS}(\Theta)$ and $\hat{R}_{LP}(\Theta)$ of $R(\Theta)$ estimates were derived from the following expressions under SELF and PLF, respectively:

$$\hat{R}_{LS}(\Theta) = \mathbb{E}(R(\Theta)|\underline{x}, \underline{y}) = \int_0^\infty \int_0^\infty R(\Theta)\pi(\Theta|\underline{x}, \underline{y})d\Theta,$$

and

$$\hat{R}_{LP}(\Theta) = \sqrt{\mathbb{E}(R^2(\Theta)|\underline{x}, \underline{y})} = \left(\int_0^\infty \int_0^\infty R^2(\Theta)\pi(\Theta|\underline{x}, \underline{y})d\Theta\right)^{\frac{1}{2}}.$$

Demonstration of the above terms and other derivatives are shown in Appendix A.1 and A.2 in details.

4.1.1. Bayesian estimates of R under SELF

According to Appendix A.1, A.2, and Equation (2.8), the Bayes estimator of $R(\Theta)$ under the SELF, given the parametric function $R(\Theta) = \dfrac{\alpha}{\theta+\alpha} + \dfrac{\theta\alpha(1-\lambda)}{(\theta+\alpha)(\theta\lambda+\alpha)}e^{-(\theta+\alpha)(e^{\tau}-1)}$ can be obtained from the following approximation:

$$\begin{aligned}\hat{R}_{LS}(\Theta) = \hat{R}_{ML} + \frac{1}{2}\Big[&(R_{\theta\theta} + 2R_{\theta}\rho_{\theta})\sigma_{\theta\theta} + (R_{\lambda\theta} + 2R_{\lambda}\rho_{\theta})\sigma_{\lambda\theta} + (R_{\alpha\alpha} + 2R_{\alpha}\rho_{\alpha})\sigma_{\alpha\alpha} \\ &+ (R_{\theta\lambda} + 2R_{\theta}\rho_{\lambda})\sigma_{\theta\lambda} + (R_{\lambda\lambda} + 2R_{\lambda}\rho_{\lambda})\sigma_{\lambda\lambda}\Big] + \frac{1}{2}\Big[\sigma_{\theta\theta}\ell_{\theta\theta\theta}(R_{\theta}\sigma_{\theta\theta} + R_{\lambda}\sigma_{\theta\lambda}) \\ &+ \sigma_{\alpha\alpha}\ell_{\alpha\alpha\alpha}(R_{\alpha}\sigma_{\alpha\alpha}) + \sigma_{\lambda\lambda}\ell_{\lambda\lambda\lambda}(R_{\theta}\sigma_{\lambda\theta} + R_{\lambda}\sigma_{\lambda\lambda})\Big].\end{aligned} \tag{4.6}$$

The subsequent parametric function derivatives that will replace those in Equation (4.6) were provided as follows:

$$\begin{array}{lll} R_{\theta} = \frac{\partial R}{\partial\theta} = A_{\theta} + B_{\theta}C + C_{\theta}B, & R_{\theta\theta} = \frac{\partial^2 R}{\partial\theta^2} = A_{\theta\theta} + 2B_{\theta}C_{\theta} + B_{\theta\theta}C + C_{\theta\theta}B, & \\ R_{\alpha} = \frac{\partial R}{\partial\alpha} = A_{\alpha} + B_{\alpha}C + C_{\alpha}B, & R_{\alpha\alpha} = \frac{\partial^2 R}{\partial\alpha^2} = A_{\alpha\alpha} + 2B_{\alpha}C_{\alpha} + B_{\alpha\alpha}C + C_{\alpha\alpha}B, & . \\ R_{\lambda} = \frac{\partial R}{\partial\lambda} = B_{\lambda}C, \quad R_{\lambda\lambda} = \frac{\partial^2 R}{\partial\lambda^2} = B_{\lambda\lambda}C, & R_{\lambda\theta} = R_{\theta\lambda} = \frac{\partial^2 R}{\partial\lambda\partial\theta} = B_{\lambda\theta}C + C_{\theta}B_{\lambda}. & \end{array} \tag{4.7}$$

4.1.2. Bayesian estimates of R under PLF

The Bayes estimator of R under the PLF, given the parametric function $R(\Theta) = \left(\dfrac{\alpha}{\theta+\alpha} + \dfrac{\theta\alpha(1-\lambda)}{(\theta+\alpha)(\theta\lambda+\alpha)}e^{-(\theta+\alpha)(e^{\tau}-1)}\right)^2$, considering Appendix A.1, A.2 and Equation (2.8), can be provided employing the following approximation:

$$\begin{aligned}\hat{R}_{LP}(\Theta) = \Bigg(\hat{R}_{ML} + \frac{1}{2}\Big[&(R_{\theta\theta} + 2R_{\theta}\rho_{\theta})\sigma_{\theta\theta} + (R_{\lambda\theta} + 2R_{\lambda}\rho_{\theta})\sigma_{\lambda\theta} + (R_{\alpha\alpha} + 2R_{\alpha}\rho_{\alpha})\sigma_{\alpha\alpha} \\ &+ (R_{\theta\lambda} + 2R_{\theta}\rho_{\lambda})\sigma_{\theta\lambda} + (R_{\lambda\lambda} + 2R_{\lambda}\rho_{\lambda})\sigma_{\lambda\lambda}\Big] + \frac{1}{2}\Big[\sigma_{\theta\theta}\ell_{\theta\theta\theta}(R_{\theta}\sigma_{\theta\theta} + R_{\lambda}\sigma_{\theta\lambda}) \\ &+ \sigma_{\alpha\alpha}\ell_{\alpha\alpha\alpha}(R_{\alpha}\sigma_{\alpha\alpha}) + \sigma_{\lambda\lambda}\ell_{\lambda\lambda\lambda}(R_{\theta}\sigma_{\lambda\theta} + R_{\lambda}\sigma_{\lambda\lambda})\Big]\Bigg)^{\frac{1}{2}}.\end{aligned} \tag{4.8}$$

The following parametric function derivatives will substitute those in Equation (4.8):

$$\begin{aligned}
&R_\theta = \tfrac{\partial R}{\partial \theta} = 2[A + BC][A_\theta + B_\theta C + C_\theta B],\\
&R_{\theta\theta} = \tfrac{\partial^2 R}{\partial \theta^2} = 2\Big[[A_\theta + B_\theta C + C_\theta B]^2 + [A + BC][A_{\theta\theta} + B_{\theta\theta} C + 2B_\theta C_\theta + C_{\theta\theta} B]\Big],\\
&R_\alpha = \tfrac{\partial R}{\partial \alpha} = 2[A + BC][A_\alpha + B_\alpha C + C_\alpha B],\\
&R_{\alpha\alpha} = \tfrac{\partial^2 R}{\partial \alpha^2} = 2\Big[[A_\alpha + B_\alpha C + C_\alpha B]^2 + [A + BC][A_{\alpha\alpha} + B_{\alpha\alpha} C + 2B_\alpha C_\alpha + C_{\alpha\alpha} B]\Big],\\
&R_\lambda = \tfrac{\partial R}{\partial \lambda} = 2[A + BC][B_\lambda C], \qquad R_{\lambda\lambda} = \tfrac{\partial^2 R}{\partial \lambda^2} = 2\Big[[B_\lambda C]^2 + [B_{\lambda\lambda} C][A + BC]\Big],\\
&R_{\lambda\theta} = R_{\theta\lambda} = \tfrac{\partial^2 R}{\partial \lambda \partial \theta} = 2\Big[[A_\theta + (B_\theta C + C_\theta B)]\Big[B_\lambda C\Big] + [B_{\lambda\theta} C + C_\theta B_\lambda][A + BC]\Big].
\end{aligned} \tag{4.9}$$

4.2. Bayesian estimates of R using the MCMC approach

Computing the analytical expression for the posterior marginal distribution function can be difficult, which poses a barrier when using the Bayesian technique for statistical inference. In this sub-section, the BEs of θ, α, and λ have been taken into consideration, utilizing SELF and PLF and making use of the Gibbs sampling method suggested by Geman and Geman [26] (for recent studies refere to, [2, 39]). The main advantage of the Gibbs sampling technique is its simplicity in execution and the tendency of its iterations to converge. The Bayes estimate of R, represented as $\hat{R}_{BSGS}$, can be derived as the mean of the posterior function, as outlined below.

The posterior conditional distributions of parameters θ, α, and λ are proportional to the following, considering Equation (4.3):

$$\begin{aligned}
\pi^*(\theta|\lambda, \underline{x}) &\propto \theta^{n+a_1-1} e^{-\theta\{b_1 + \sum_{i=1}^{r}(e^{x_i}-1) + \sum_{i=r+1}^{n}[\lambda(e^{x_i}-e^{\tau}) + (e^{\tau}-1)]\}},\\
\pi^*(\alpha|\underline{y}) &\propto \alpha^{m+a_2-1} e^{-\alpha\{b_2 + \sum_{j=1}^{m}(e^{y_j}-1)\}},\\
\pi^*(\lambda|\theta, \underline{x}) &\propto \lambda^{n-r-1} e^{-\lambda\{\theta \sum_{i=r+1}^{n}(e^{x_i}-e^{\tau})\}}.
\end{aligned}$$

The MCMC approach has been employed to generate a sample with the Gibbs sampling algorithm to obtain the Bayesian estimates of the SSP R, as outlined in Algorithm 1: as follows:

Algorithm 1 : Bayes estimate of R based on Gibbs sampling approach

1. Assign starting values to the unknown parameters θ, α, and λ, represented as $\theta^{(o)}, \alpha^{(o)}$ and $\lambda^{(o)}$.
2. Set ν=1.
3. Generate $\theta^{(\nu)}$ from Gamma $(n + a_1, b_1 + \sum_{i=1}^{r}(e^{x_i} - 1) + \sum_{i=r+1}^{n}[\lambda(e^{x_i} - e^{\tau}) + (e^{\tau} - 1)])$.
4. Generate $\alpha^{(\nu)}$ from Gamma $(m + a_2, b_2 + \sum_{j=1}^{m}(e^{y_j} - 1))$.
5. Generate $\lambda^{(\nu)}$ from Gamma $(n - r, \theta \sum_{i=r+1}^{n}(e^{x_i} - e^{\tau}))$.
6. Set $\nu = \nu + 1$.
7. Compute $R_B^{(\nu)}$ at $\theta^{(\nu)}, \alpha^{(\nu)}$, and $\lambda^{(\nu)}$.
8. Perform iterations 2-7 multiple times for a total of ν. Then, store the values of $R_B^{(\nu)}$ for each iteration, where ν ranges from 1 to N. In order to achieve convergence and mitigate the impact of initial value selection, ignore the first M iterations to account for the burn-in period.

Under the guidance of SELF, compute Bayesian estimate values of the parameter R. The following is the formula for each of these parameters in the sequence in which they are defined:

$$\hat{R}_{GS} = \frac{1}{N - M} \sum_{i=M+1}^{N} R_B^{(\nu)}.$$

Using PLF, Bayesian estimates for the SSP R were computed by applying the following formula:

$$\hat{R}_{GP} = \left[\frac{1}{N-M}\sum_{i=M+1}^{N} R_B^{(\nu)}\right]^{\frac{1}{2}}.$$

5. E-Bayes Estimate of *R*

As a consequence of the difficulty in identifying the hyperparameters, there is a certain degree of unpredictability involved in the process. In this particular scenario, E-BEs are derived by calculating the average of the Bayes estimates of Θ using hyperparameters a_i and b_i in the domain D. This section will study the E-Bayes estimate of θ and α using SELF and PLF, given λ as a known parameter. Estimation was considered in the following manner:

$$\hat{\Theta}_{EBE} = E[\hat{\Theta}_{BE}(a_i, b_i)] = \int_D\int \hat{\Theta}_{BE}(a_i, b_i)S(\Theta|a_i, b_i)da_i db_i, \qquad i = 1, 2. \tag{5.1}$$

As stated by Han [28], it is necessary to select a_i and b_i in a way to ensure that $S(\Theta|a_i, b_i)$ is a decreasing function of Θ.

$$\frac{\partial S(\Theta|a_i, b_i)}{\partial\Theta_i} = \frac{b_i^{a_i}}{\Gamma(a_i)}\Theta_i^{a_i-2}e^{-\Theta_i b_i}[(a_i-1)-b_i\Theta_i].$$

Thus, the hyperparameters a_i and b_i should be in the ranges $0 < a_i < 1$; $b_i > 0$, due to $\frac{\partial S(\Theta|a_i,b_i)}{\partial\Theta_i} < 0$ and therefore $S(\Theta|a_i, b_i)$ is a decreasing function of Θ. As b_i bounds increase, the gamma density function's tail becomes thinner, resulting in low probability for extreme values. The thinner-tailed prior distribution often leads to a decrease in the robustness of Bayesian estimation, as discussed by Berger [12]. Consequently, b_i must not exceed a specified upper limit c, where $c > 0$ is a constant to be determined. Consequently, it is obligatory to select hyperparameters a_i and b_i within the constraints of $0 < a < 1$ and $0 < b < c$.

Referring to Zhang et al. [52], two distinct prior distributions of the hyperparameters a_i and b_i have been assigned to examine the impact of these various distributions on E-BEs of Θ. These distributions are shown below as follows:

$$\begin{aligned} S_1(a_i, b_i) &= \tfrac{1}{cB(W,V)}a_i^{W-1}(1-a_i)^{V-1} \\ S_2(a_i, b_i) &= \tfrac{2}{c^2B(W,V)}(c-b_i)a_i^{W-1}(1-a_i)^{V-1} \end{aligned} \quad . \tag{5.2}$$

The following subsections discuss E-BEs utilizing the Lindley approximation method and the MCMC approach, assuming the parameter λ is known.

5.1. E-Bayesian estimation of R using Lindley approximation method

To obtain E-BEs, we need to obtain the expected values of ρ_θ and ρ_α given by Equation (A.1.1) in Apendix A.1 over the prior distributions of the hyperparameters given by Equation (4.9), respectively.

(i) **Expectation of $\rho_{\theta.\iota}$ under $S_\iota(a_1, b_1)$, where $\iota = 1, 2$.**

$$\begin{aligned}\rho_{\theta.1} &= \int_0^c \int_0^1 \rho_\theta S_1(a_1, b_1)\, da_1\, db_1 \\ &= \int_0^c \int_0^1 \left[\frac{(a_1-1)}{\theta} - b_1\right] \frac{1}{cB(W,V)} a_1^{W-1}(1-a_1)^{V-1}\, da_1\, db_1 \\ &= \frac{1}{\theta}\left[\frac{W}{W+V} - 1 - \frac{c\theta}{2}\right],\end{aligned} \tag{5.3}$$

and,

$$\begin{aligned}\rho_{\theta.2} &= \int_0^c \int_0^1 \rho_\theta S_2(a_1, b_1)\, da_1\, db_1 \\ &= \int_0^c \int_0^1 \left[\frac{(a_1-1)}{\theta} - b_1\right] \frac{2}{c^2B(W,V)} (c-b_1) a_1^{W-1}(1-a_1)^{V-1}\, da_1\, db_1 \\ &= \frac{1}{\theta}\left[\frac{W}{W+V} - 1 - \frac{c\theta}{3}\right].\end{aligned} \tag{5.4}$$

(ii) **Expectation of $\rho_{\alpha.\imath}$ under $S_\imath(a_2, b_2)$, where $\imath = 1, 2$.**

$$\begin{aligned}\rho_{\alpha.1} &= \int_0^c \int_0^1 \rho_\alpha S_1(a_2, b_2)\, da_2\, db_2 \\ &= \int_0^c \int_0^1 \left[\frac{(a_2-1)}{\alpha} - b_2\right] \frac{1}{cB(W,V)} a_2^{W-1}(1-a_2)^{V-1}\, da_2\, db_2 \\ &= \frac{1}{\alpha}\left[\frac{W}{W+V} - 1 - \frac{c\alpha}{2}\right],\end{aligned} \tag{5.5}$$

and,

$$\begin{aligned}\rho_{\alpha.2} &= \int_0^c \int_0^1 \rho_\alpha S_2(a_2, b_2)\, da_2\, db_2 \\ &= \int_0^c \int_0^1 \left[\frac{(a_2-1)}{\alpha} - b_2\right] \frac{2}{c^2B(W,V)} (c-b_2) a_2^{W-1}(1-a_2)^{V-1}\, da_2\, db_2 \\ &= \frac{1}{\alpha}\left[\frac{W}{W+V} - 1 - \frac{c\alpha}{3}\right].\end{aligned} \tag{5.6}$$

5.1.1. E-Bayesian estimates of R under SELF

Now, the different E-BE of $R(\Theta)$, say $\hat{R}_{EBSEL}(\Theta)$, can be obtained employing Lindley approximation methods under SELF by substituting Equations from (5.4) to (5.6) in Equation (4.5), assuming the parametric function $R(\Theta) = \dfrac{\alpha}{\theta+\alpha} + \dfrac{\theta\alpha(1-\lambda)}{(\theta+\alpha)(\theta\lambda+\alpha)} e^{-(\theta+\alpha)(e^{\tau}-1)}$, and considering Appendix A.1 and

A.2 as follows:

$$\begin{aligned}\hat{R}_{ELSS_\iota}(\theta,\alpha,\lambda) = \hat{R}_{ML} + \frac{1}{2}\Big[&(R_{\theta\theta}+2R_\theta\rho_{\theta.\iota})\sigma_{\theta\theta}+(R_{\lambda\theta}+2R_\lambda\rho_{\theta.\iota})\sigma_{\lambda\theta}+(R_{\alpha\alpha}+2R_\alpha\rho_{\alpha.\iota})\sigma_{\alpha\alpha}\\ &+(R_{\theta\lambda}+2R_\theta\rho_\lambda)\sigma_{\theta\lambda}+(R_{\lambda\lambda}+2R_\lambda\rho_\lambda)\sigma_{\lambda\lambda}\Big]+\frac{1}{2}\Big[\sigma_{\theta\theta}\ell_{\theta\theta\theta}(R_\theta\sigma_{\theta\theta}+R_\lambda\sigma_{\theta\lambda})\\ &+\sigma_{\alpha\alpha}\ell_{\alpha\alpha\alpha}(R_\alpha\sigma_{\alpha\alpha})+\sigma_{\lambda\lambda}\ell_{\lambda\lambda\lambda}(R_\theta\sigma_{\lambda\theta}+R_\lambda\sigma_{\lambda\lambda})\Big],\end{aligned} \tag{5.7}$$

where, $\iota = (1,2) \equiv (S_1(a_i,b_i), S_2(a_i,b_i))$.

5.1.2. E-Bayesian estimates of R under PLF

Similarly, E-BE under PLF can be obtained by substituting Equations from (5.4) to (5.6) in Equation (4.5), taking into account Appendix A.1 and A.2, and assuming the parametric function $R(\Theta) = \left(\frac{\alpha}{\theta+\alpha} + \frac{\theta\alpha(1-\lambda)}{(\theta+\alpha)(\theta\lambda+\alpha)}e^{-(\theta+\alpha)(e^\tau-1)}\right)^2$ as follows:

$$\begin{aligned}\hat{R}_{ELPS_\iota}(\theta,\alpha,\lambda) = \Bigg(\hat{R}_{ML} + \frac{1}{2}\Big[&(R_{\theta\theta}+2R_\theta\rho_{\theta.\iota})\sigma_{\theta\theta}+(R_{\lambda\theta}+2R_\lambda\rho_{\theta.\iota})\sigma_{\lambda\theta}+(R_{\alpha\alpha}+2R_\alpha\rho_{\alpha.\iota})\sigma_{\alpha\alpha}\\ &+(R_{\theta\lambda}+2R_\theta\rho_\lambda)\sigma_{\theta\lambda}+(R_{\lambda\lambda}+2R_\lambda\rho_\lambda)\sigma_{\lambda\lambda}\Big]+\frac{1}{2}\Big[\sigma_{\theta\theta}\ell_{\theta\theta\theta}(R_\theta\sigma_{\theta\theta}+R_\lambda\sigma_{\theta\lambda})\\ &+\sigma_{\alpha\alpha}\ell_{\alpha\alpha\alpha}(R_\alpha\sigma_{\alpha\alpha})+\sigma_{\lambda\lambda}\ell_{\lambda\lambda\lambda}(R_\theta\sigma_{\lambda\theta}+R_\lambda\sigma_{\lambda\lambda})\Big]\Bigg)^{\frac{1}{2}},\end{aligned} \tag{5.8}$$

where, $\iota = (1,2) \equiv (S_1(a_i,b_i), S_2(a_i,b_i))$.

The parametric function's derivatives, given by Equations (4.7) and (4.8), will replace those in Equations (5.7) and (5.8), respectively. Appendix A.1 and A.2 provide a detailed explanation of the terms mentioned above as well as other derivatives.

5.2. E-Bayesian estimation of R's parameters using the MCMC approach

Algorithm 2 demonstrates the use of the MCMC method with the Gibbs sampling technique to obtain the E-Bayesian estimates of the SSP R as outlined below:

Algorithm 2: E-Bayes estimate of R based on Gibbs sampling approach

1. Assign initial values to the unknown parameters θ, α, and λ. Assigned parameters are represented as $\theta^{(o)}$, $\alpha^{(o)}$, and $\lambda^{(o)}$.
2. Set the values of c, W, and V.
3. Set ν=1.
4. Generate samples from the Beta distribution $a_i^{(\nu)} \sim B(W,V)$ and uniform distribution $b_i^{(\nu)} \sim U(0,c)$ as stated by Equation (5.2).
5. Generate $\theta^{(\nu)}$ from Gamma $(n+a_1^{(\nu)}, b_1^{(\nu)} + \sum_{i=1}^r (e^{x_i}-1) + \sum_{i=r+1}^n [\lambda(e^{x_i}-e^\tau)+(e^\tau-1)])$.
6. Generate $\alpha^{(\nu)}$ from Gamma $(m+a_2^{(\nu)}, b_2^{(\nu)} + \sum_{j=1}^m (e^{y_j}-1))$.

continued on the next page

continued from the previous page

Algorithm 2: E-Bayes estimate of R based on Gibbs sampling approach

7. Generate $\lambda^{(\nu)}$ from Gamma $(n-r, \theta\sum_{i=r+1}^{n}(e^{x_i}-e^{\tau}))$.
8. Set $\nu=\nu+1$.
9. Compute $R_{EB_\iota}^{(\nu)}$ at $\theta^{(\nu)}, \alpha^{(\nu)}$ and $\lambda^{(\nu)}$.
10. Repeat iterations from 2-9 many times until a total of N iterations have been completed. Next, record the values of $R_{EB_\iota}^{(\nu)}$ for every iteration, with N ranging from 1 to N. To achieve convergence and minimize the influence of initial value selection, discard the first M iterations as burn-in.

The formulas for each of the R_{EB} parameters are listed below, represented as R_{EBSGS} under the SELF and R_{EBPGS} under the PLF.

$$\hat{R}_{EGSS_\iota}=\frac{1}{N-M}\sum_{i=M+1}^{N}R_{EB_\iota}^{(\nu)},$$

and

$$\hat{R}_{EGPS_\iota}=\left[\frac{1}{N-M}\sum_{i=M+1}^{N}R_{EB_\iota}^{(\nu)}\right]^{\frac{1}{2}}.$$

6. Interval Estimation

This section proposes constructing the ACIs using the asymptotic features of maximum likelihood estimators of θ and α. For the parameters θ and α, credible intervals are obtained using the MCMC simulated variations of the BEs and E-BEs.

6.1. Approximate confidence intervals

The 100 $(1-\Phi)\%$ ACIs for Θ, where $\Theta\equiv(\theta,\alpha,\lambda)$, can be estimated using the inverse of the observed FIM $I(\hat{\Theta})$ given in Equation (A.1.2) of Appendix A.1. To be exact, σ_{ij} represents the $(i,j)^{th}$ element of the ℓ_{ij} inverse matrix, all evaluated at MLE of parameters.

$$I^{-1}(\hat{\Theta})=\begin{bmatrix}-\ell_{\theta\theta} & -\ell_{\theta\alpha} & -\ell_{\theta\lambda}\\ -\ell_{\alpha\theta} & -\ell_{\alpha\alpha} & -\ell_{\alpha\lambda}\\ -\ell_{\lambda\theta} & -\ell_{\lambda\alpha} & -\ell_{\lambda\lambda}\end{bmatrix}^{-1}=\begin{pmatrix}\hat{\sigma}_{\theta\theta} & \hat{\sigma}_{\theta\alpha} & \hat{\sigma}_{\theta\lambda}\\ \hat{\sigma}_{\alpha\theta} & \hat{\sigma}_{\alpha\alpha} & \hat{\sigma}_{\alpha\lambda}\\ \hat{\sigma}_{\lambda\theta} & \hat{\sigma}_{\lambda\alpha} & \hat{\sigma}_{\lambda\lambda}\end{pmatrix}. \tag{6.1}$$

The second partial derivatives ℓ_{ij}, $i=(1,2,3)\equiv(\theta,\alpha,\lambda)$, and $j=(1,2,3)\equiv(\theta,\alpha,\lambda)$ are previously reported in subsection (4.1). Under some mild regularity conditions, maximum likelihood estimators of θ, α and λ are approximately distributed as normal distribution $\hat{\theta}\sim N(\theta,\sigma_{\theta\theta})$, $\hat{\alpha}\sim N(\theta,\sigma_{\alpha\alpha})$ and $\hat{\lambda}\sim N(\theta,\sigma_{\lambda\lambda})$, respectively. To construct the 100 $(1-\Phi)\%$ of ACIs of the SSP R, we need to approximate the variance estimate of it.

The delta method, which is a general approach to obtain the approximate estimates of the variance associated with maximum likelihood estimators of the SSP R is used for this purpose; for more details, see [43]. However, according to the delta method based on Equation (6.1), the variance of R obtained at their maximum likelihood estimators θ and α can be approximated as:

$$\hat{\sigma}^2_{\hat{R}} = [\triangledown \hat{R}]^T I^{-1}(\hat{\Theta})[\triangledown \hat{R}]|_{(\theta,\alpha,\lambda)=(\hat{\theta},\hat{\alpha},\hat{\lambda})}, \tag{6.2}$$

where $\triangledown \hat{R}$ is the gradients of R with respect to θ, α, and λ, as

$$[\triangledown R]^T = \left[\frac{\partial R}{\partial \theta}, \frac{\partial R}{\partial \alpha}, \frac{\partial R}{\partial \lambda}\right].$$

Finally, substituting Equation (6.1) in Equation (6.2), the following formula is obtained:

$$\hat{\sigma}^2_{\hat{R}} = \left(\frac{\partial R}{\partial \theta}\right)^2 \hat{\sigma}_{\theta\theta} + \left(\frac{\partial R}{\partial \alpha}\right)^2 \hat{\sigma}_{\alpha\alpha} + \left(\frac{\partial R}{\partial \lambda}\right)^2 \hat{\sigma}_{\lambda\lambda} + 2\left(\frac{\partial R}{\partial \theta}\frac{\partial R}{\partial \lambda}\right)\hat{\sigma}_{\theta\lambda}.$$

Hence, the 100 $(1-\Phi)$% two-sided ACI for any function of R obtained based on $\hat{R}$ is given by:

$$\hat{R} \pm Z_{\frac{\Phi}{2}} \sqrt{\hat{\sigma}^2_{\hat{R}}},$$

where $Z_{\frac{\Phi}{2}}$ is the $(\frac{\Phi}{2})$-th upper percentile of the standard normal distribution.

6.2. *Bayes and E-Bayes credible intervals*

To construct the corresponding Bayesian and E-Bayesian credible intervals of any function of the SSP R, the associated MCMC simulated obtained in Subsections (4.2 and 5.2) are used, respectively. To construct the BCIs, order the simulated samples of Bayesian MCMC estimates $R^{(N)}$ for $N = 1, 2, ..., M$ after burn-in M_o as $R^{(M_o+1)}, R^{(M_o+2)}, ..., R^{(M)}$. Hence, the 100 $(1-\Phi)$% two-sided BCIs of R is given by:

$$\left(R_{(M-M_o)(\frac{\Phi}{2})}, R_{(M-M_o)(1-(\frac{\Phi}{2}))}\right).$$

Similarly, the 100 $(1-\Phi)$% two-sided E-Bayesian MCMC estimates for R can be easily constructed.

7. Real Data Application

This section examines the datasets that were first described by Efron [21] . The data collection encompasses two distinct groups of persons diagnosed with head and neck cancer. The initial dataset displays the survival time of 58 individuals diagnosed with head and neck cancer who underwent radiation therapy. Conversely, the second dataset delineates the survival time of 44 patients who received both radiation treatment and chemotherapy. The subsequent information has been compiled:
Radio (X): 523, 583, 594, 14.48, 16.1, 22.7, 34, 41.55, 42, 45.28, 49.4, 84, 91, 160, 160, 165, 108, 112, 129, 133, 133, 139, 140, 140, 146, 149, 154, 157, 146, 149, 154, 157, 160, 160, 165, 173, 176, 218, 6.53, 7, 10.42, 225, 241, 248, 273, 277, 297, 405, 417, 53.62, 63, 64, 83, 420, 440, 1101, 1146, 1417.
Radio and chemotherapy (Y): 25.87, 31.98, 37, 41.35, 47.38, 55.46, 58.36, 63.47, 319, 339, 432, 469, 68.46, 78.26, 173, 179, 194, 195, 74.47, 81.43, 84, 92, 519, 633, 725, 94, 110, 112, 119, 127, 130, 133, 140, 146, 12.2, 23.56, 23.74, 155, 159, 209, 249, 281, 817, 1776.
Transformation has been carried out upon data by dividing both sets by 20000. The estimated parameter, log-likelihood values, Cramér–von Mises criterion (CVM), Kolmogorov-Smirnov (K-S) distances, and corresponding p-values are presented for the datasets in Table 1.

Table 1. Parameters, log-likelihood, CVM, K-S distances, and p-values of the fitted GD to radio (X) and radio and chemotherapy datasets (Y).

Data Set	Estimated		Log-Likelihood	CVM	K-S distances	p-Value
	Parameters	Values				
Radio (X)	θ λ	0.151 592.171	203.350	0.258	0.172	0.056
Radio and chemotherapy (Y)	α	88.077	153.533	0.190	0.149	0.255

Table 1 shows that goodness of fitness statistics indicate the GD is appropriate for both real datasets. Although the log-likelihood suggests that the radio (X) dataset may initially appear to fit the model better, CVM and K-S distances and p-value statistics consistently favor the combined treatment radio and chemotherapy (Y) dataset.

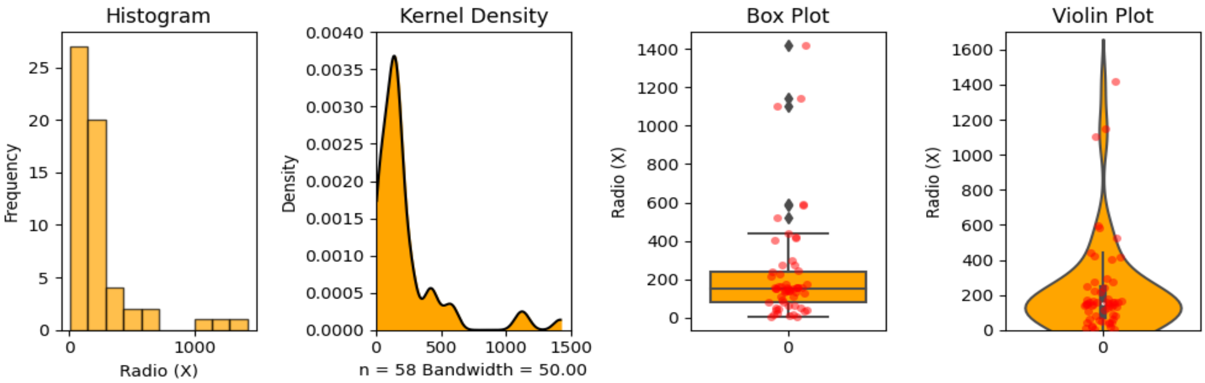

Figure 4. Some non-parametric plots for radio (X) dataset.

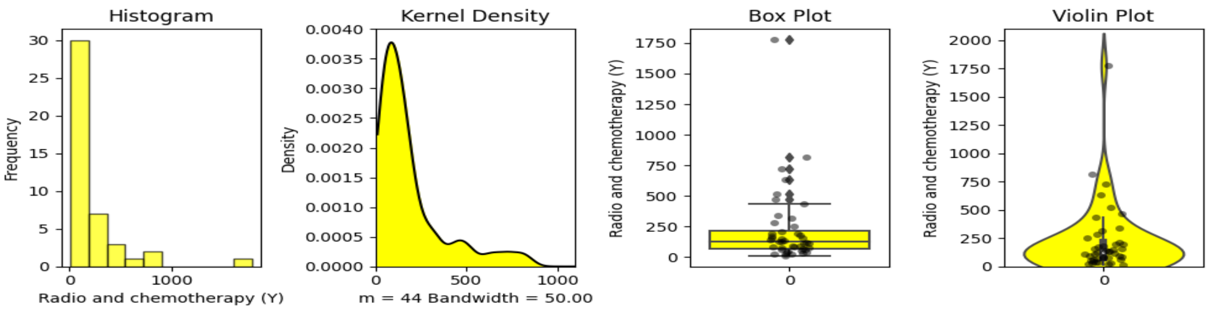

Figure 5. Some non-parametric plots for the radio and chemotherapy (Y) dataset.

Figures 4 and 5 pertaining to the original datasets indicate that the probability density function shapes depicted through non-parametric kernel density plots corroborate the right skewness evident in the histogram, with peak density occurring at lower values (approximately 50–100) in both datasets. The box plot identified the outliers, demonstrating their presence in both datasets, and the tiny interquartile range suggests that most data points are proximate to the median. In the violin plot, the wide portion in the plot indicates that most of the data points are clustered in that range (0, 200) and (0, 250) for radio (X) and radio and chemotherapy (Y) datasets, respectively. Moving higher across the y-axis, the violin narrows significantly, indicating fewer data points in those regions.

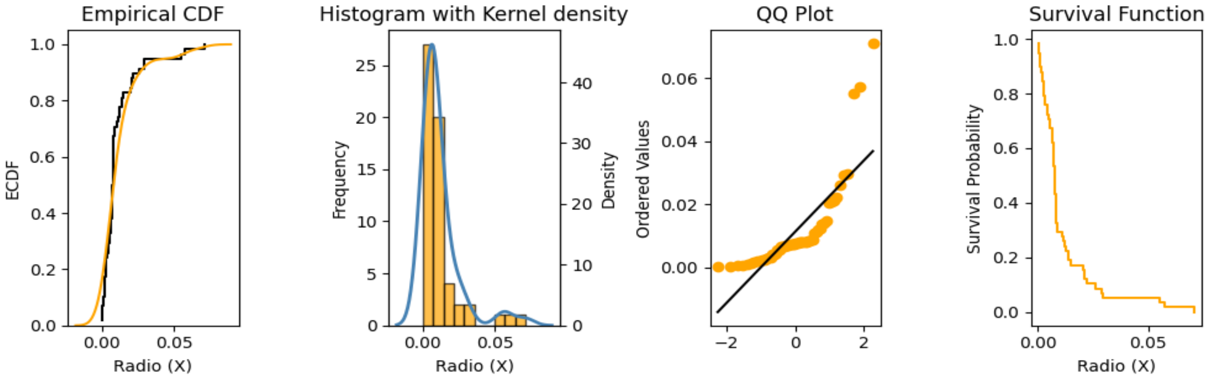

Figure 6. Empirical CDF, histograms with Gaussian kernel density, Q-Q, and survival function plots for radio (X) dataset after transformation.

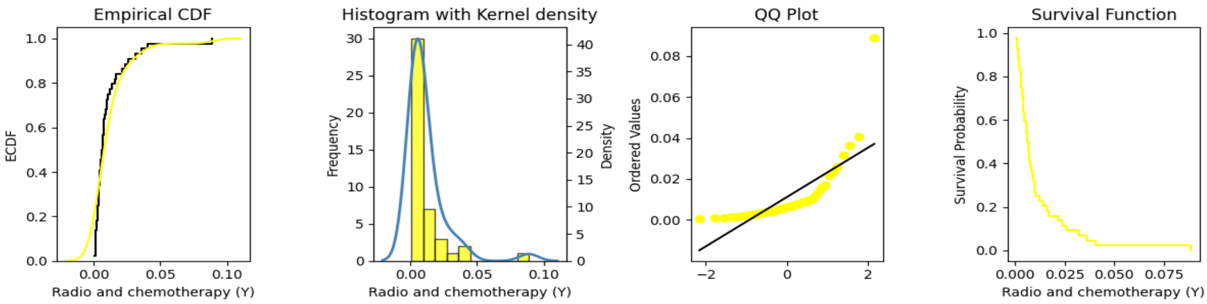

Figure 7. Empirical CDF, histograms with Gaussian kernel density, Q-Q, and survival function plots for radio and chemotherapy (Y) dataset after transformation.

Based on the evidence shown in Figures 6 and 7, the empirical CDF and the theoretical CDF are highly aligned, indicating that the theoretical distribution well describes the sets of data, as well as the histogram with kernel density plot. The quantile-quantile (Q-Q) plot indicates that the dataset has a skewed or heavy-tailed distribution, making normality assumptions invalid.

The estimation of SSP varies with the stress change time τ, consistent with the implementation of SSPALT for the strength variable. In this case, τ is set to 0.01. Using the real data previously mentioned above, the MLE of R is $\hat{R}_{ML} = 0.440023$, with an ACI of $(0.363526, 0.516520)$, a length of 0.152995, and a coverage probability (CP) of 100%. To calculate the Bayesian estimates of R, prior distributions for the parameters θ, α, and λ are defined. Take $a_i = b_i = 0.0001$ (for $i = 1, 2$) of the hyperparameters for θ and α (see [19]) for more details. Lindley's approximation method, in addition to the Gibbs sampling technique, is applied to generate 5000 MCMC samples for posterior analysis. For the SELF, the Bayesian estimate $\hat{R}_{LS}$ is calculated as 0.440032 using Lindley's approximation method. Under the PLF, $\hat{R}_{LP}$ is determined to be 0.663349. Using the Gibbs sampling method, the MCMC simulation yields $\hat{R}_{GS} = 0.472392$ under SELF, with a 95% credible interval of $(0.373293, 0.570910)$, a length of 0.197617, and CP of 95.0%. For PLF, the corresponding Gibbs sampling result is $\hat{R}_{GP} = 0.687308$. The E-Bayesian estimation approach utilizes Lindley's approximation to determine prior distributions for the hyperparameters $S_\iota(a_i, b_i)$ (for $\iota, i = 1, 2$), with parameters $W = 0.2$, $V = 0.3$, and $c = 0.1$. SELF-based E-Bayesian estimates are $\hat{R}_{ELSS_\iota} = 0.440057$ and 0.440048, while PLF-based estimates are R_{ELPS_ι} = 0.663368 and 0.663361. Using Gibbs sampling for E-Bayesian estimation under SELF, the estimated values $\hat{R}_{EGSS_\iota}$ are 0.477689 and 0.477588, with 95% credible intervals of (0.370849, 0.583826) and (0.365000, 0.592551), lengths of 0.212977 and 0.227551, and a CP of 95.0%. For PLF, the corresponding estimates are $\hat{R}_{EGPS_\iota}$ = 0.691150 and 0.691077.

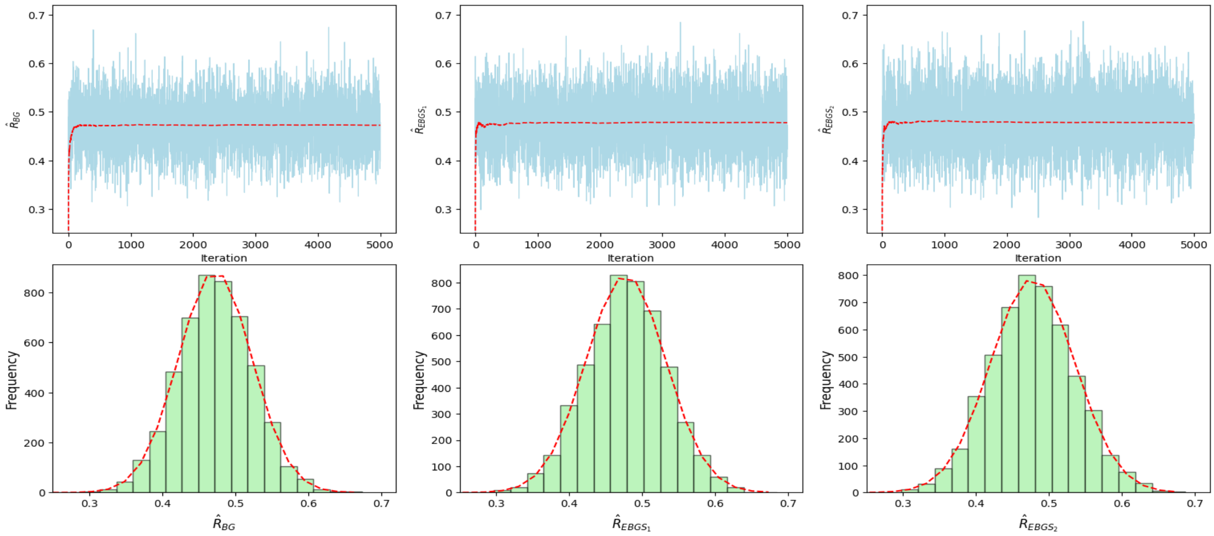

Figure 8. Trace and posterior density with normal curve for MCMC results under SELF for Efron data.

Trace graphs for the MCMC outputs of R are presented in Figure 8, demonstrating satisfactory convergence of the MCMC technique. Furthermore, the histogram plots of the generated samples indicate a strong alignment with the theoretical posterior density functions.

8. Simulation Studies

To illustrate the behavior of the SSP R, various combinations of initial parameter values (θ, α, λ, and τ) and differing sample sizes were simulated in Python for 5000 iterations to compute the average performance of the proposed estimators. The effectiveness of maximum likelihood estimators, Bayesian and E-Bayesian estimators, as well as ACIs, Bayes, and E-Bayes credible intervals, based on Lindley's approximation method and MCMC simulation, have been evaluated in terms of mean square error (MSE), length, and CP. Within the context of E-Bayesian estimation, the estimation of λ is derived by the Bayesian estimation technique. A comprehensive sample comprises a random sample of size n representing the strength component of the GD with parameters θ and λ, denoted as $x_1, x_2, \ldots, x_n$, alongside a random sample of size m for the stress component from GD with parameter α, represented as $y_1, y_2, \ldots, y_m$. The examined sample sizes are (n, m) = (50, 50), (50, 35), and (90, 90) across different scenarios of true parameter values, stress change times, and acceleration factors. The cases are enumerated as follows:

- Case I: θ=1.8, α=0.6, λ=2.5, τ=0.4, a_1, a_2, b_1, b_2=0.001 , W=0.8, V=1.5, and c=0.5.

- Case II: θ=1.8, α=3.5, λ=2.5, τ=0.4, a_1, a_2, b_1, b_2=0.001 , W=0.8, V=1.5, and c=0.5.

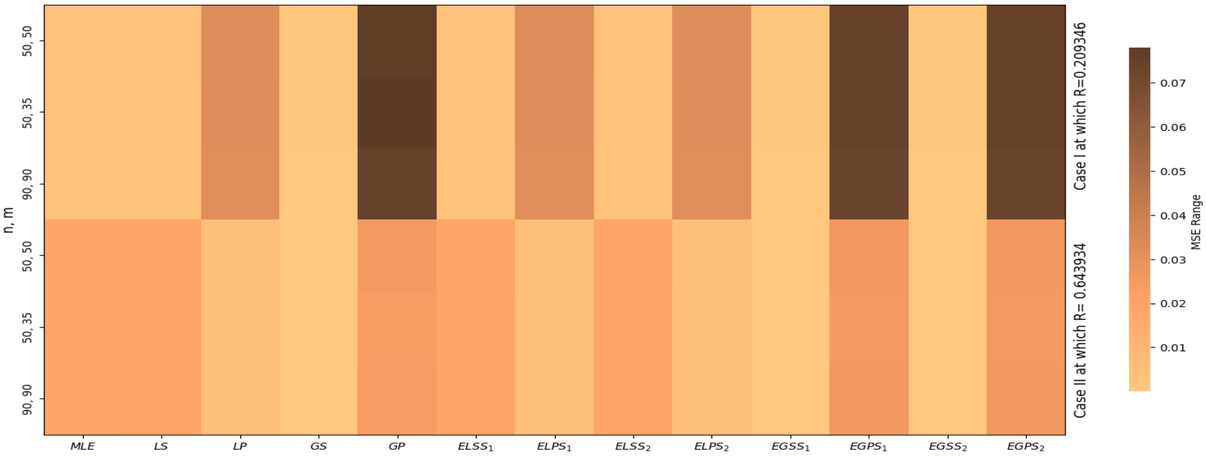

Figure 9. The heatmaps of the simulated R of the MLE, Bayesian, and E-Bayesian estimation under Lindley's approximation method and MCMC simulation.

The simulation results of point and interval estimates were summarized in Tables B.1.1 - B.1.4 and B.2.1-B.2.2 in Appendix (B), yielding the following observations:

1. Estimates of R for sample size (n, m) = (50, 50) and (90, 90) exhibit the property of consistency; that is, the MSE decreases as the sample size increases.

2. All estimates of R possess highly accurate values that are theoretically comparable.

3. While the MCMC method involves higher computational complexity due to its iterative nature, the significant reduction in MSE justifies the additional computation time compared to Lindley's approximation method.

4. Bayesian and E-Bayesian estimates utilizing the MCMC approach provide accurate R estimation with reduced MSE in comparison to Bayesian and E-Bayesian estimation employing Lindley's approximation method.

5. In all cases, Bayesian and E-Bayesian estimates have MSE values that are roughly equal across all sample sizes (n, m).

6. In all cases, Bayesian and E-Bayesian estimates under SELF have lower MSE compared to those under PLF for all sample sizes (n, m).

7. According to the heatmap in Figure 9, all estimation methods at the true value of Case II demonstrate a lower MSE than those in Case I, except for the MLE, as well as Bayesian and E-Bayesian estimation utilizing Lindley's approximation method under SELF.

8. Heatmap analysis illustrated a strong dependency between parameter combinations and estimator performance. The visual patterns indicate that under certain parameter settings, Bayesian estimators demonstrated their full potential. While in the case of lowering the initial value of α (Case I), the MSE across most of the estimation methods widened significantly.

9. A high CP% indicates that the estimates of CIs, including Bayesian and E-Bayesian estimation, are more effective than those of ACI.

10. The CP% of the interval estimates in Case I, takes the largest values except for the ACI estimates compared to the true value of Case II.

9. Conclusion

This study makes a significant contribution to the literature by providing a deeper understanding of how the stress variable, modeled by $GD(\alpha)$, influences the strength variables governed by $GD(\theta)$ and $GD(\theta, \lambda)$ within the framework of $R = P(Y < X)$ under SSPALT. Through a combination of the Lindley approximation method with Gibbs sampling, alongside SELF and PLF employing INF and NINF priors, E-Bayesian estimation, and E-BCIs of R have been computed to enhance computational precision and ensure a comprehensive and rigorous analysis. In addition to that contribution, the observed FIM was formulated to calculate the ACI, and the maximum likelihood estimation of R was derived. The Bayesian estimate of R and its credible interval have been obtained. The precision of the data provided is validated by a comprehensive simulation study. All estimates are capable of producing very accurate results; E-BCIs outperform all other Bayes CIs in terms of CP. Real-world data representing stress and strength variables have been evaluated using MLE, Bayesian, and E-Bayesian methods. In future research, it would be interesting to analyze the estimation concerns of the same model adopted in the current study in the presence of other censoring schemes and different estimation techniques such as hierarchical Bayesian estimation.

Appendix A

A.1. Determine the theoretical components of the Lindley's approximation formula.

In our estimation problem, we calculate the approximate Bayes estimates of θ, α, and λ utilizing Equation (4.6), and we assess the relevant expressions as follows:

$$\rho = \log S(\Theta) \propto (a_1 - 1)\log(\theta) + (a_2 - 1)\log(\alpha) - \theta b_1 - \alpha b_2 - \log(\lambda)$$

Later on, we obtain:

$$\rho_\theta = \frac{\partial \rho}{\partial \theta} = \frac{(a_1 - 1)}{\theta} - b_1; \qquad \rho_\alpha = \frac{\partial \rho}{\partial \alpha} = \frac{(a_2 - 1)}{\alpha} - b_2; \qquad \rho_\lambda = \frac{\partial \rho}{\partial \lambda} = -\frac{1}{\lambda}. \tag{A.1.1}$$

The observed FIM matrix is written as:

$$I(\hat{\Theta}) = -\begin{bmatrix} \frac{\partial^2 \ell(\Theta|\underline{x},\underline{y})}{\partial \theta^2} & \frac{\partial^2 \ell(\Theta|\underline{x},\underline{y})}{\partial \theta \partial \alpha} & \frac{\partial^2 \ell(\Theta|\underline{x},\underline{y})}{\partial \theta \partial \lambda} \\ \frac{\partial^2 \ell(\Theta|\underline{x},\underline{y})}{\partial \alpha \partial \theta} & \frac{\partial^2 \ell(\Theta|\underline{x},\underline{y})}{\partial \alpha^2} & \frac{\partial^2 \ell(\Theta|\underline{x},\underline{y})}{\partial \alpha \partial \lambda} \\ \frac{\partial^2 \ell(\Theta|\underline{x},\underline{y})}{\partial \lambda \partial \theta} & \frac{\partial^2 \ell(\Theta|\underline{x},\underline{y})}{\partial \lambda \partial \alpha} & \frac{\partial^2 \ell(\Theta|\underline{x},\underline{y})}{\partial \lambda^2} \end{bmatrix}_{(\hat{\theta},\hat{\alpha},\hat{\lambda})} = \begin{pmatrix} -\ell_{\theta\theta} & -\ell_{\theta\alpha} & -\ell_{\theta\lambda} \\ -\ell_{\alpha\theta} & -\ell_{\alpha\alpha} & -\ell_{\alpha\lambda} \\ -\ell_{\lambda\theta} & -\ell_{\lambda\alpha} & -\ell_{\lambda\lambda} \end{pmatrix}. \tag{A.1.2}$$

Hence, ℓ_{ij} is acquired in the following manner for $i, j = 1, 2, 3$:

$$\ell_{\theta\theta} = -\frac{n}{\theta^2}; \qquad \ell_{\theta\lambda} = -\sum_{i=r+1}^{n} (e^{x_i} - e^{\tau}); \qquad \ell_{\alpha\alpha} = -\frac{m}{\alpha^2}; \qquad \ell_{\lambda\lambda} = -\frac{(n-r)}{\lambda^2}. \tag{A.1.3}$$

Given Equation (A.1.3), the subsequent results were deduced concerning σ_{ij} as follows:

$$\begin{aligned}
\sigma_{\theta\theta} &= -\frac{\ell_{\lambda\lambda}}{\ell_{\theta\theta}\ell_{\lambda\lambda}-(\ell_{\theta\lambda})^2} = \frac{n-r}{\frac{n(n-r)}{\theta^2}-\left(\lambda\sum_{i=r+1}^{n}(e^{x_i}-e^{\tau})\right)^2},\\
\sigma_{\theta\lambda} &= \frac{\ell_{\theta\lambda}}{\ell_{\theta\theta}\ell_{\lambda\lambda}-(\ell_{\theta\lambda})^2} = -\frac{\sum_{i=r+1}^{n}(e^{x_i}-e^{\tau})}{\frac{n(n-r)}{\theta^2\lambda^2}-\left(\sum_{i=r+1}^{n}(e^{x_i}-e^{\tau})\right)^2},\\
\sigma_{\alpha\alpha} &= -\frac{1}{\ell_{\alpha\alpha}} = \frac{\alpha^2}{m},\\
\sigma_{\lambda\lambda} &= -\frac{\ell_{\theta\theta}}{\ell_{\theta\theta}\ell_{\lambda\lambda}-(\ell_{\theta\lambda})^2} = \frac{n}{\frac{n(n-r)}{\lambda^2}-\left(\theta\sum_{i=r+1}^{n}(e^{x_i}-e^{\tau})\right)^2}.
\end{aligned} \tag{A.1.4}$$

The values of ℓ_{ijk} are derived as follows for $i, j, k = 1, 2, 3$:

$$\ell_{\theta\theta\theta} = \frac{2n}{\theta^3}; \qquad \ell_{\alpha\alpha\alpha} = \frac{2m}{\alpha^3}; \qquad \ell_{\lambda\lambda\lambda} = \frac{2(n-r)}{\lambda^3}. \tag{A.1.5}$$

It was definitely worth emphasizing that $\ell_{\theta\alpha} = \ell_{\alpha\theta} = \ell_{\alpha\lambda} = \ell_{\lambda\theta} = \ell_{\lambda\alpha} = \ell_{\theta\alpha\theta} = \ell_{\theta\lambda\theta} = \ell_{\alpha\lambda\theta} = \ell_{\alpha\alpha\theta} = \ell_{\lambda\lambda\theta} = \ell_{\theta\theta\alpha} = \ell_{\theta\alpha\alpha} = \ell_{\theta\lambda\alpha} = \ell_{\alpha\lambda\alpha} = \ell_{\lambda\lambda\alpha} = \ell_{\theta\theta\lambda} = \ell_{\theta\alpha\lambda} = \ell_{\theta\lambda\lambda} = \ell_{\alpha\lambda\lambda} = \ell_{\alpha\alpha\lambda} = \sigma_{\theta\alpha} = \sigma_{\alpha\theta} = \sigma_{\alpha\lambda} = \sigma_{\lambda\alpha} = 0$.

A.2. Determine the parametric functions and their related differentiated terms under SELF and PLF.

Given the parametric function under SELF, $R = A + BC$, considering its related terms $A = \dfrac{\alpha}{\theta+\alpha}$, $B = \dfrac{\theta\alpha(1-\lambda)}{(\theta+\alpha)(\theta\lambda+\alpha)}$, and $C = e^{-(\theta+\alpha)(e^{\tau}-1)}$. Thus, the partial differentiation of these terms will be given as follows:

(1) The first partial derivative with respect to θ.

$$A_{\theta} = -\frac{\alpha}{(\theta+\alpha)^2}; \quad B_{\theta} = \frac{\alpha(1-\lambda)(\alpha^2-\theta^2\lambda)}{(\theta+\alpha)^2(\theta\lambda+\alpha)^2}; \quad C_{\theta} = -(e^{\tau}-1)e^{-(\theta+\alpha)(e^{\tau}-1)}. \tag{A.2.1}$$

(2) The second partial derivative with respect to θ.

$$\begin{aligned}
A_{\theta\theta} &= \frac{2\alpha}{(\theta+\alpha)^3}\\
B_{\theta\theta} &= -\frac{2\alpha(1-\lambda)\left[\theta\lambda(\theta+\alpha)(\theta\lambda+\alpha)+(\alpha^2-\theta^2\lambda)(\alpha+\alpha\lambda+2\theta\lambda)\right]}{(\theta+\alpha)^3(\theta\lambda+\alpha)^3}\\
C_{\theta\theta} &= (e^{\tau}-1)^2 e^{-(\theta+\alpha)(e^{\tau}-1)}
\end{aligned} \tag{A.2.2}$$

(3) The first partial derivative with respect to α.

$$A_{\alpha} = \frac{\theta}{(\theta+\alpha)^2}; \quad B_{\alpha} = \frac{\theta(1-\lambda)(\theta^2\lambda-\alpha^2)}{(\theta+\alpha)^2(\theta\lambda+\alpha)^2}; \quad C_{\alpha} = -(e^{\tau}-1)e^{-(\theta+\alpha)(e^{\tau}-1)}. \tag{A.2.3}$$

(4) The second partial derivative with respect to α.

$$\begin{aligned}
A_{\alpha\alpha} &= -\frac{2\theta}{(\theta+\alpha)^3}\\
B_{\alpha\alpha} &= -\frac{2\theta(1-\lambda)\left[\theta\alpha\lambda(2\alpha-\theta)-\theta^3\lambda(1+\lambda)+\alpha^2(2\theta+3\alpha)\right]}{(\theta+\alpha)^3(\theta\lambda+\alpha)^3}\\
C_{\alpha\alpha} &= (e^{\tau}-1)^2 e^{-(\theta+\alpha)(e^{\tau}-1)}
\end{aligned} \tag{A.2.4}$$

(5) The first and the second partial derivative with respect to λ.

$$B_\lambda = -\frac{\theta\alpha}{(\theta\lambda+\alpha)^2}; \quad B_{\lambda\lambda} = \frac{2\theta^2\alpha}{(\theta\lambda+\alpha)^3}. \tag{A.2.5}$$

(6) The second-order partial derivative with respect to θ, after taking the first derivative with respect to λ.

$$B_{\lambda\theta} = \frac{\alpha(\theta\lambda-\alpha)}{(\theta\lambda+\alpha)^3} = B_{\theta\lambda}. \tag{A.2.6}$$

Appendix B

B.1. Average estimates (first row), biases (second row), and MSE (third rows)

Table B.1.1. Initial values involves θ=1.8, α=0.6, λ=2.5, τ=0.4, $a_1 = a_2$=2, $b_1 = b_2$=1, and actual R=0.209346.

n, m	**MLE**	**Bayesian estimation**			
		Lindley's approximation method		**MCMC method**	
		SELF	**PLF**	**SELF**	**PLF**
50, 50	0.151070	0.151117	0.389125	0.234376	0.482437
	-0.058276	-0.058229	0.179778	0.025029	0.273090
	0.003396	0.003391	0.032320	0.000626	0.074578
50, 35	0.152374	0.152422	0.389077	0.234313	0.482825
	-0.056972	-0.056925	0.179731	0.024967	0.273479
	0.003246	0.003240	0.032303	0.000623	0.074791
90, 90	0.152755	0.152231	0.388068	0.231273	0.480199
	-0.056591	-0.057115	0.178721	0.021927	0.270853
	0.003203	0.003262	0.031941	0.000481	0.073361

Table B.1.2. Initial values involves θ=1.8, α=3.5, λ=2.5, τ=0.4, $a_1 = a_2$=2, $b_1 = b_2$=1, and actual R=0.643934.

n, m	**MLE**	**Bayesian estimation**			
		Lindley's approximation method		**MCMC method**	
		SELF	**PLF**	**SELF**	**PLF**
50, 50	0.507919	0.507424	0.712212	0.653524	0.807832

Continued on next page

Table B.1.2– *Continued from previous page*

n, m	MLE	Bayesian estimation			
		Lindley's approximation method		MCMC method	
		SELF	PLF	SELF	PLF
	-0.136014	-0.136509	0.068278	0.009590	0.163898
	0.018500	0.018635	0.004662	0.000092	0.026863
50, 35	0.509102	0.507843	0.711770	0.651516	0.806305
	-0.134832	-0.136090	0.067837	0.007582	0.162372
	0.018180	0.018521	0.004602	0.000057	0.026365
90, 90	0.509300	0.508155	0.711832	0.652456	0.807414
	-0.134633	-0.135779	0.067898	0.008523	0.163480
	0.018126	0.018436	0.004610	0.000073	0.026726

Table B.1.3. Initial values involves θ=1.8, α=0.6, λ=2.5, τ=0.4, W=0.8, V=1.5, c=0.5, and actual R=0.209346.

n, m	E-Bayesian estimation							
	Lindley's approximation method				MCMC method			
	$S_1(\theta,\alpha)$		$S_2(\theta,\alpha)$		$S_1(\theta,\alpha)$		$S_2(\theta,\alpha)$	
	SELF	PLF	SELF	PLF	SELF	PLF	SELF	PLF
50, 50	0.151143	0.389206	0.151151	0.389233	0.236284	0.484420	0.236245	0.484384
	-0.058203	0.179859	-0.058195	0.179887	0.026938	0.275074	0.026898	0.275038
	0.003388	0.032349	0.003387	0.032359	0.000726	0.075666	0.000724	0.075646
50, 35	0.152484	0.389157	0.152506	0.389184	0.235432	0.483988	0.235438	0.483998
	-0.056862	0.179811	-0.056840	0.179837	0.026086	0.274642	0.026092	0.274652
	0.003233	0.032332	0.003231	0.032342	0.000680	0.075428	0.000681	0.075434
90, 90	0.152295	0.388100	0.152317	0.388111	0.231765	0.480719	0.231834	0.480787
	-0.057051	0.178754	-0.057029	0.178765	0.022419	0.271373	0.022488	0.271441
	0.003255	0.031953	0.003252	0.031957	0.000503	0.073643	0.000506	0.073680

Table B.1.4. Initial values involves θ=1.8, α=3.5, λ=2.5, τ=0.4, W=0.8, V=1.5, c=0.5, and actual R=0.643934.

n, m	E-Bayesian estimation							
	Lindley's approximation method				MCMC method			
	$S_1(\theta,\alpha)$		$S_2(\theta,\alpha)$		$S_1(\theta,\alpha)$		$S_2(\theta,\alpha)$	
	SELF	**PLF**	**SELF**	**PLF**	**SELF**	**PLF**	**SELF**	**PLF**
50, 50	0.507594	0.712451	0.507649	0.712531	0.651563	0.806625	0.651564	0.806627
	-0.136340	0.068518	-0.136285	0.068597	0.007630	0.162691	0.007630	0.162694
	0.018589	0.004695	0.018574	0.004706	0.000058	0.026468	0.000058	0.026469
50, 35	0.508181	0.712007	0.508293	0.712085	0.649168	0.804865	0.649083	0.804814
	-0.135752	0.068073	-0.135640	0.068152	0.005234	0.160931	0.005149	0.160881
	0.018429	0.004634	0.018398	0.004645	0.000027	0.025899	0.000027	0.025883
90, 90	0.508497	0.711951	0.508610	0.711989	0.651193	0.806636	0.651269	0.806682
	-0.135437	0.068017	-0.135323	0.068056	0.007260	0.162702	0.007335	0.162748
	0.018343	0.004626	0.018312	0.004632	0.000053	0.026472	0.000054	0.026487

B.2. Upper bound (first rows), lower bound (second rows), average range (third rows), length (fourth rows), and Coverage Probability (fifth rows) of the estimates

Table B.2.1. Initial values involve θ=1.8, α=0.6, λ=2.5, τ=0.4, $a_1 = a_2$=2, $b_1 = b_2$=1, W=0.8, V=1.5, c=0.5 , and actual R=0.209346.

n, m	ACI	BCIs	E-BCIs	
			$S_1(\theta,\alpha)$	$S_2(\theta,\alpha)$
50, 50	0.12612	0.18723	0.17337	0.17322
	0.17625	0.28518	0.30573	0.30591
	0.05013	0.09794	0.13236	0.13269
	4.82	83.68	88.94	88.94
50, 35	0.11176	0.17181	0.16703	0.16692
	0.19349	0.31783	0.31405	0.31410
	0.08173	0.14602	0.14701	0.14718
	28.58	88.36	90.92	90.92
90, 90	0.11886	0.17700	0.18520	0.18516
	0.18602	0.30840	0.28332	0.28336
	0.06715	0.13140	0.09812	0.09820
	18.92	87.00	86.00	86.00

Table B.2.2. Initial values involve θ=1.8, α=3.5, λ=2.5, τ=0.4, $a_1 = a_2$=2, $b_1 = b_2$=1, W=0.8, V=1.5, c=0.5 , and actual R=0.643934.

n, m	ACI	BCIs	E-BCIs	
			$S_1(\theta, \alpha)$	$S_2(\theta, \alpha)$
50, 50	0.45460	0.54945	0.57836	0.57820
	0.56409	0.73472	0.71960	0.71968
	0.10950	0.18527	0.14124	0.14148
	2.80	94.80	93.26	93.26
50, 35	0.43831	0.53457	0.54051	0.54009
	0.57973	0.73712	0.74579	0.74599
	0.14142	0.20255	0.20528	0.20591
	9.12	95.28	94.74	94.74
90, 90	0.46633	0.57587	0.55351	0.55328
	0.54965	0.71657	0.74107	0.74130
	0.08332	0.14070	0.18756	0.18802
	0.26	94.20	93.70	93.70

References

1. Abushal, T.A., and Soliman, A.A. (2015). Estimating the Pareto parameters under progressive censoring data for constant-partially accelerated life tests. Journal of Statistical Computation and Simulation, 85(5), 917–934. https://doi.org/10.1080/00949655.2013.853768
2. Albadawy, A., Ashour, E., EL-Helbawy, A., and AL-Dayian, G. (2024). Bayesian estimation and prediction for exponentiated inverted Topp-Leone distribution. Computational Journal of Mathematical and Statistical Sciences, 3(1), 33–56. https://doi.org/10.21608/cjmss.2023.241890.1022
3. Alomani, G.A., Hassan, A.S., Al-Omari, A.I., and Almetwally, E.M. (2024). Different estimation techniques and data analysis for constant-partially accelerated life tests for power half-logistic distribution. Scientific Reports, 14(1), 20865. https://doi.org/10.1038/s41598-024-71498-w
4. Alsadat, N., Hassan, A. S., Elgarhy, M., Muhammad, M., and Almetwally, E. M. (2024). Reliability inference of a multicomponent stress-strength model for exponentiated Pareto distribution based on progressive first failure censored samples. Journal of Radiation Research and Applied Sciences, 17, 101122. https://doi.org/10.1016/j.jrras.2024.101122
5. Alrashidi, A., Rabie, A., Mahmoud, A. A., Nasr, S. G., Mustafa, M. S., Al Mutairi, A., Hussam, E., and Hossain, M. M. (2024). Exponentiated gamma constant-stress partially accelerated life tests with unified hybrid censored data: Statistical inferences. Alexandria Engineering Journal, 88, 268–275. https://doi.org/10.1016/j.aej.2023.12.066
6. Amleh, M. A., and Al-Freihat, I. F. (2024). Estimations with step-stress partially accelerated life tests for Ailamujia distribution under Type-I censored data. International Journal of Analysis and Applications, 22, 22–55.

7. Almetwally, E. M., Khaled, O. M., & Barakat, H. M. (2025). Inference Based on Progressive-Stress Accelerated Life-Testing for Extended Distribution via the Marshall-Olkin Family Under Progressive Type-II Censoring with Optimality Techniques. Axioms, 14(4), 244.
8. Asadi, S., and Panahi, H. (2022). Estimation of stress–strength reliability based on censored data and its evaluation for coating processes. Quality Technology and Quantitative Management, 19(3), 379–401.
9. Asadi, S., Panahi, H., Swarup, C., and Lone, S.A. (2022). Inference on adaptive progressive hybrid censored accelerated life test for Gompertz distribution and its evaluation for virus-containing micro droplets data. Alexandria Engineering Journal, 61(12), 10071–10084.
10. Asgharzadeh, A., Valiollahi, R., and Raqab, M. Z. (2013). Estimation of the stress–strength reliability for the generalized logistic distribution. Statistical Methodology, 15, 73–94. https://doi.org/10.1016/j.stamet.2013.05.002
11. Bemmaor, A.C., and Glady, N. (2012). Modeling purchasing behavior with sudden "death: A flexible customer lifetime model. Management Science, 58(5), 1012–1021.
12. Berger, J. O. (2013). Statistical decision theory and Bayesian analysis. Springer Science and Business Media.
13. Bhattacharyya, G. K., and Soejoeti, Z. (1989) A tampered failure rate model for step-stress accelerated life test. Communications in Statistics-Theory and Methods 18(5), 1627–1643.
14. Birnbaum, Z.W. (1956). On a use of the Mann-Whitney statistics. In Proceedings of the Third Berkeley Symposium on Mathematical Statistics and Probability 1, 13–17.
15. Birnbaum, Z.W., and McCarty, R.C. (1958). A distribution-free upper confidence bound for $P(Y < X)$, based on independent samples of X and Y. The Annals of Mathematical Statistics, 29(2), 558–562.
16. Brown, K. S., and Forbes, W. F. (1974). A mathematical model of aging processes. Journal of Gerontology, 29 (1), 46–51. https://doi.org/10.1093/geronj/29.1.46
17. Carlin, B.P., and Louis, T.A. (2000). Empirical Bayes: Past, present and future. Journal of the American Statistical Association 95(452), 1286–1289.
18. Çetinkaya, Ç. (2021) The stress-strength reliability model with component strength under partially accelerated life test. Communications in Statistics-Simulation and Computation, 52(10), 4665–4684.
19. Congdon, P. (2014). Applied Bayesian Modelling. John Wiley and Sons.
20. Economos, A. C. (1982). Rate of aging, rate of dying, and the mechanism of mortality. Archives of Gerontology and Geriatrics, 1 (1), 3–27.
21. Efron, B. (1988). Logistic regression, survival analysis, and the Kaplan-Meier curve. Journal of the American Statistical Association, 83 (402), 414–425. https://doi.org/10.1080/01621459.1988.10478612
22. Eliwa, M. S., and Ahmed, E. A. (2023). Reliability analysis of constant partially accelerated life tests under progressive first-failure type-II censored data from Lomax model: EM and MCMC algorithms. AIMS Mathematics, 8(1), 29–60. https://doi.org/10.3934/math.2023002

23. El-Gohary, A., Alshamrani, A., and Al-Otaibi, A. N. (2013). The generalized Gompertz distribution. Applied Mathematical Modelling, 37(1-2), 13–24.

24. El-Sagheer, R. M., Tolba, A. H., Jawa, T. M., and Sayed-Ahmed, N. (2022). Inferences for stress-strength reliability model in the presence of partially accelerated life tests to its strength variable. Computational Intelligence and Neuroscience, 2022 (1), 4710536. https://doi.org/10.1155/2022/4710536

25. Fayomi, A., Hassan, A. S., and Almetwally, E. A. (2025). Reliability inference for multicomponent systems based on the inverted exponentiated Pareto distribution and progressive first-failure censoring. Journal of Nonlinear Mathematical Physics, 32 (12). https://doi.org/10.1007/s44198-024-00262-5

26. Geman, S., and Geman, D. (1984). Stochastic relaxation, Gibbs distributions, and the Bayesian restoration of images. IEEE Transactions on Pattern Analysis and Machine Intelligence, 6 (6), 721–741. https://doi.org/10.1109/TPAMI.1984.4767596

27. Gompertz, B. (1825). On the nature of the function expressive of the law of human mortality, and on a new mode of determining the value of life contingencies. In a letter to Francis Baily, Esq. FRS and c. Philosophical Transactions of the Royal Society of London, 115, 513–583, https://doi.org/10.1098/rstl.1825.0026.

28. Han, M. (1997). The structure of hierarchical prior distribution and its applications. Chinese Operations Research and Management Science, 6(3), 31–40.

29. Hassan, A.S., and Morgan, Y.S. (2025). Stress-strength reliability inference for exponentiated half-logistic distribution containing outliers. Quality & Quantity, 59, 275–311, https://doi.org/10.1007/s11135-024-01927-5

30. Hassan, A.S., and Morgan, Y.S. (2025). Bayesian and non-Bayesian analysis of $R = Pr(W < Q < Z)$ for inverted Kumaraswamy distribution containing outliers with data application. Quality & Quantity. https://doi.org/10.1007/s11135-025-02097-8

31. Hassan, A. S., Pramanik, S., Maiti, S., and Nassr, S.G. (2020). Estimation in constant stress partially accelerated life tests for Weibull distribution based on censored competing risks data. Annals of Data Science, 7(1), 45–62.

32. Hassan, A. S., Hagag, A. E., Metwally, N., and Sery, O. (2025). Statistical analysis of inverse Weibull based on step-stress partially accelerated life tests with unified hybrid censoring data. Computational Journal of Mathematical and Statistical Sciences, 4(1), 162–185. https://doi.org/10.21608/cjmss.2024.319502.1072

33. Johnson, N.L., Kotz, S., and Balakrishnan, N. (1995). Continuous Univariate Distributions. Volume 2 (Vol. 289). John Wiley and Sons.

34. Kamal, M., Rahman, A., Zarrin, S., and Kausar, H. (2021). Statistical inference under step stress partially accelerated life testing for adaptive type-II progressive hybrid censored data. Journal of Reliability and Statistical Studies, 14(2), 585–614.

35. Kumar, S., and Vaish, M. (2017). A study of strength-reliability for Gompertz distributed stress. International Journal of Statistics and System, 12(3), 567–574.

36. Lindley, D.V. (1980). Approximate Bayesian methods. Trabajos de Estadística e Investigación Operativa, 31(1), 223–245.
37. Madi, M.T. (1993). Multiple step-stress accelerated life test: the tampered failure rate model. Communications in Statistics-Theory and Methods, 22(9), 295–306.
38. Moheb, S., Hassan, A.S., and Diab, L.S. (2024). Classical and Bayesian inferences of stress-strength reliability model based on record data. Communications for Statistical Applications and Methods, 31, 497–519.
39. Mohamed, A.A., Refaey, R.M., and AL-Dayian, G.R. (2024). Bayesian and E-Bayesian estimation for odd generalized exponential inverted Weibull distribution. Journal of Business and Environmental Sciences, 3(2), 275–301. https://doi.org/10.21608/jcese.2024.288853.1061
40. Moheb, S., Hassan, A. S., and Diab, L.S. (2025). Inference of $P(X < Y < Z)$ for unit exponentiated half-logistic distribution with upper record ranked set samples. Sankhya A: The Indian Journal of Statistics. https://doi.org/10.1007/s13171-025-00380-2
41. Mokhlis, N.A. (2005). Reliability of a stress-strength model with Burr type III distributions. Communications in Statistics-Theory and Methods, 34(7), 1643–1657.
42. Norstrom, J. G. (1996). The use of precautionary loss functions in risk analysis. IEEE Transactions on Reliability, 45(3), 400–403. https://doi.org/10.1109/24.536992
43. Oehlert, G. W. (1992). A note on the delta method. The American Statistician, 46(1), 27–29. https://doi.org/10.1080/00031305.1992.10475842
44. Ohishi, K., Okamura, H., and Dohi, T. (2009). Gompertz software reliability model: Estimation algorithm and empirical validation. Journal of Systems and Software, 82(3), 535–543.
45. Saraçoğlu, B., and Kaya, M.F. (2007). Maximum likelihood estimation and confidence intervals of system reliability for Gompertz distribution in stress-strength models. Selçuk Journal of Applied Mathematics, 8(2), 25–36.
46. Sarhan, A.M., and Tolba, A.H. (2023) Stress-strength reliability under partially accelerated life testing using Weibull model. Scientific African 20, e01733. https://doi.org/10.1016/j.sciaf.2023.e01733
47. Srivastava, P.W., and Mittal, N. (2010). Optimum step-stress partially accelerated life tests for the truncated logistic distribution with censoring. Applied Mathematical Modelling, 34(10), 3166–3178.
48. Temraz, N. S. Y. (2024). Fuzzy multicomponent stress-strength reliability in presence of partially accelerated life testing under generalized progressive hybrid censoring scheme subject to inverse Weibull model. MethodsX, 12, 102586. https://doi.org/10.1016/j.mex.2024.102586
49. Wang, J., and Guo, X. (2024). The Gompertz model and its applications in microbial growth and bioproduction kinetics: Past, present and future. Biotechnology Advances, 108335. https://doi.org/10.1016/j.biotechadv.2024.108335
50. Willemse, W.J., and Koppelaar, H. (2000). Knowledge elicitation of Gompertz'law of mortality. Scandinavian Actuarial Journal, 2000 (2), 168–179, https://doi.org/10.1080/034612300750066845.

51. Yousef, M.M., Fayomi, A., and Almetwally, E.M. (2023). Simulation techniques for strength component partially accelerated to analyze stress–strength model. Symmetry 15(6), 1183. https://doi.org/10.3390/sym15061183
52. Zhang, Y., Liu, K., and Gui, W. (2021). Bayesian and E-Bayesian estimations of bathtub-shaped distribution under generalized Type-I hybrid censoring. Entropy, 23(8), 934. https://doi.org/10.3390/e23080934